

The Functionalization of MOF-5 with Hexamethylenetetramine for CO₂ Capture



By

Muhammad Akram

(Registration No: 00000402872)

Department of Energy Systems Engineering

U.S-Pakistan Centre for Advanced Studies in Energy

National University of Sciences & Technology (NUST)

Islamabad, Pakistan

(2025)

The Functionalization of MOF-5 with Hexamethylenetetramine for CO₂ Capture



By

Muhammad Akram

(Registration No: 00000402872)

A thesis submitted to the National University of Sciences and Technology, Islamabad,

in partial fulfillment of the requirements for the degree of

Master of Science in

Energy Systems Engineering

Supervisor: Prof. Dr. Naseem Iqbal

U.S-Pakistan Centre for Advanced Studies in Energy (USPCAS-E)

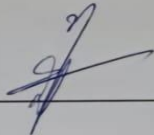
National University of Sciences & Technology (NUST)

Islamabad, Pakistan

(2025)

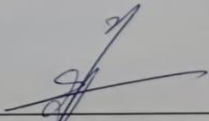
THESIS ACCEPTANCE CERTIFICATE

Certified that final copy of MS thesis written by Mr. Muhammad Akram, (Registration No. 402872), of U.S Pakistan Center for Advanced Studies in Energy has been vetted by undersigned, found complete in all respects as per NUST Statues/Regulations, is within the similarity indices limit and is accepted as partial fulfillment for the award of Master's degree. It is further certified that necessary amendments as pointed out by GEC members and foreign/ local evaluators of the scholar have also been incorporated in the said thesis.


Signature: 

Name of Supervisor: Dr. Naseem Iqbal

Date: 09-01-2025

Signature (HOD): 

Date: 09-01-2025

Signature (Dean/ Principal): 

Date: 14/01/2025

National University of Sciences & Technology
MASTER'S THESIS WORK

We hereby recommend that the dissertation prepared under our supervision by (Student Name & Regn No.) Muhammad Akram, 00000402872

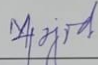
Titled: The functionalization of MOF-5 with hexamethylenetetramine for CO₂ Capture in partial fulfillment of the requirements for the award of MS Energy Systems Engineering degree with (A grade).

Examination Committee Members

1. Name Dr. Nadia Shahzad

Signature: 

2. Name Dr. Majid Ali

Signature: 

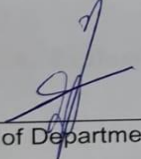
3. Name Dr. Mustafa Anwar

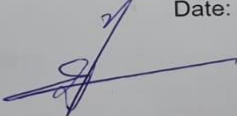
Signature: 

Supervisor's name: Dr. Naseem Iqbal

Signature: 

Date: 07-01-2025

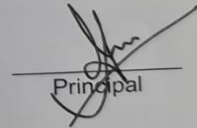

 Head of Department


 Signature

07-01-2025
 Date

COUNTERSIGNED

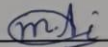
Date: 14/01/2025


 Principal

CERTIFICATE OF APPROVAL

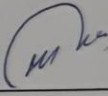
This is to certify that the research work presented in this thesis, entitled "The Functionalization of MOF-5 with Hexamethylenetetramine for CO₂ capture" was conducted by Muhammad Akram under the supervision of Dr. Naseem Iqbal. No part of this thesis has been submitted anywhere else to any other degree. This thesis is submitted to the US-Pakistan Center for Advanced Studies in Energy (USPCAS-E), in partial fulfillment of the requirements for the degree of Master of Science in Field of Energy Systems Engineering, Department of Energy Systems Engineering, National University of Sciences and Technology, Islamabad.

Student Name: Muhammad Akram

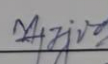
Signature: 

Examination Committee:

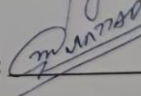
a) GEC Member 1: Dr. Nadia Shahzad
Associate Professor, USPCAS-E

Signature: 

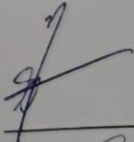
b) GEC Member 2: Dr. Majid Ali
Associate Professor, USPCAS-E

Signature: 

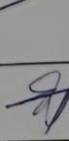
c) GEC Member 3: Dr. Mustafa Anwar
Assistant Professor, USPCAS-E

Signature: 

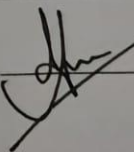
Supervisor Name: Dr. Naseem Iqbal

Signature: 

Name of HOD: Dr. Naseem Iqbal

Signature: 

Name of Principal/Dean: Dr. Adeel Waqas

Signature: 

AUTHOR'S DECLARATION

I, Muhammad Akram, hereby state that my MS thesis titled "The Functionalization of MOFs for CO₂ Capture" is my own work and has not been submitted previously by me for taking any degree from National University of Sciences and Technology (NUST), Islamabad, or anywhere else in the country / world. At any time if my statement is found to be incorrect even after my Graduation, the university has the right to withdraw my MS degree.

Name of Student: Muhammad Akram

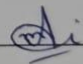
Date: 09 - 01 - 2025

PLAGIARISM UNDERTAKING

I solemnly declare that research work presented in the thesis titled “**The Functionalization of MOF-5 with Hexamethylenetetramine for CO₂ Capture**” is solely my research work with no significant contribution from any other person. Small contribution/ help wherever taken has been duly acknowledged and that complete thesis has been written by me.

I understand the zero-tolerance policy of the HEC and National University of Sciences and Technology (NUST), Islamabad towards plagiarism. Therefore, I as an author of the above titled thesis declare that no portion of my thesis has been plagiarized and any material used as reference is properly referred/cited.

I undertake that if I am found guilty of any formal plagiarism in the above titled thesis even after award of MS degree, the University reserves the rights to withdraw/revoke my MS degree and that HEC and NUST, Islamabad has the right to publish my name on the HEC/University website on which names of students are placed who submitted plagiarized thesis.

Student Signature:  _____

Name: Muhammad Akram

DEDICATION

MY PARENTS

TO WHOM I SHALL ALWAYS

REMAIN INDEBTE

ACKNOWLEDGMENTS

First of all, I want to express my heartfelt gratitude to Almighty Allah, the Creator of Everything. I also want to show my respect for His Prophet Muhammad (PBUH), to whom Allah's blessings and peace be granted. Without His guidance, completing this challenging task would not have been possible.

This dissertation marks the end of my MS journey, which has been filled with valuable lessons in scientific knowledge and research project management. I am especially thankful to my supervisor, Dr. Naseem Iqbal, for his unwavering support, helpful guidance, and research expertise. His command of scientific processes and understanding of research problems has played a crucial role in bringing this work to life.

I also want to thank my GEC members for their constant support and guidance during this research project. Their sincere comments and suggestions have brought fineness into this thesis. I am very grateful to all the faculty members and lab engineers at the U.S.-Pakistan Center for Advanced Studies in Energy (USPCAS-E), NUST, for their encouragement and assistance. A special thanks goes to Dr. Rimsha Mehek for her continuous support and helpful advice. Her willingness to share her knowledge and her encouragement to explore new ideas has been essential in completing this work. I truly appreciate her kindness and support throughout this process. I also appreciate Engineer Naveed Ahmed and Miss Neelam Zaman for their technical assistance.

I want to give special thanks to my parents and in-laws, whose prayers helped me through this challenging journey, making it easier to complete. To my beloved wife, Hafsa Akram, thank you for being by my side throughout this process. I also want to express my love and gratitude to my brothers, sister, and friends—Muhammad Tahir Kamran, Tausheen Raza, and Muhammad Ajmal. This achievement is a result of the combined efforts of everyone involved in this journey.

Muhammad Akram

TABLE OF CONTENTS

ACKNOWLEDGMENTS	viii
TABLE OF CONTENTS.....	ix
LIST OF TABLES	xi
LIST OF FIGURES	xii
LIST OF SYMBOLS, ABBREVIATIONS AND ACRONMS.....	xiv
ABSTRACT.....	xvi
CHAPTER 1: INTRODUCTION	1
1.1 CO₂ as Greenhouse Gas	1
1.2 Role of CO₂ in Global Warming.....	2
1.3 Carbon Capture & Storage	3
1.3.1 Pre-Combustion Technology.....	5
1.3.2 Post-Combustion Technology	6
1.3.3 Oxy-Flame Combustion Technology	8
1.4 CO₂ Capture by Absorbents	8
1.4.1 Metal Organic Frameworks (MOFs) for CO ₂ Capture	10
1.5 MOFs Selection Criteria.....	11
1.6 Methods for Synthesis of MOFs	12
1.6.1 Solvothermal or Hydrothermal Method	13
1.6.2 Microwave Synthesis Method.....	14
1.6.3 Electrochemical Method	15
1.6.4 Sonochemical Method.....	15
1.6.5 Spray Drying/Evaporation Method	16
1.6.6 Chemical Flow Method.....	17
1.6.7 Comparison of Different Synthesis Methodologies	17
1.7 Applications for MOFs	18
1.7.1 MOFs as a Sensor.....	19
1.7.2 MOFs for Gas Separation and Storage.....	20
1.7.3 MOFs for Drug Delivery.....	21
1.7.4 MOFs for Cancer Theragnostic.....	22
1.7.5 MOFs as a Magnetic Material.....	22
1.7.6 MOFs for Electrocatalysis.....	23
CHAPTER 2: LITERATURE REVIEW	26
2.1 DABCO based MOFs	26
2.2 Amino Functionalized MOFs	26
2.3 Benzene Tricarboxylate (BTC) based MOFs.....	26

2.4	HMTA based MOFs.....	27
2.5	MOF-5	28
2.6	MOF-199	28
2.7	MOF-74	29
2.8	UiO-66.....	29
2.9	MOF-200	30
2.10	MOF-500	30
2.11	MOF-74	31
2.12	Research Gap.....	32
2.13	Problem Statement.....	32
2.14	Research Objectives	32
CHAPTER 3: INTRODUCTION TO EXPERIMENTAL TECHNIQUES.....		33
3.1	Physiochemical Characterization Techniques.....	33
3.2	Physisorption Analysis	38
CHAPTER 4: METHODOLOGY.....		40
4.1	Materials.....	40
4.2	Equipment.....	40
4.3	Synthesis of MOFs Series.....	40
4.3.1	Zn-BDC \supset HMTA Synthesis.....	41
4.3.2	Ni-BDC \supset HMTA Synthesis	41
CHAPTER 5: RESULTS AND DISCUSSION		42
5.1	X-Ray Diffraction (XRD).....	42
5.2	Scanning Electron Microscope (SEM)	44
5.3	Fourier Transform Infrared Spectroscopy (FTIR).....	45
5.4	Thermo-Gravimetric Analysis (TGA)	49
5.5	Brunauer-Emmett-Teller Analysis (BET).....	52
5.6	X-ray Photoelectron Spectroscopy (XPS)	56
5.7	CO ₂ Adsorption Study of MOFs	58
CHAPTER 6: CONCLUSION AND FUTURE RECOMMENDATION.....		63
6.1	Conclusion.....	63
6.2	Recommendations	63
REFERENCES.....		65
LIST OF PUBLICATIONS.....		73

LIST OF TABLES

	Page No.
Table 5.1: FTIR bands corresponding to different bonds available in the Zn-BDC-HMTA MOF structure	47
Table 5.2: FTIR bands corresponding to different bonds available in the Ni-BDC-HMTA MOF structure	49
Table 5.3: CO ₂ adsorption capacity of all the zinc and nickel-based MOFs with BDC and HMTA modified MOFs at different temperature conditions	60
Table 5.4: CO ₂ adsorption capacity and BET surface area of different MOFs reported in comparison with the synthesized MOFs for this study	61

LIST OF FIGURES

	Page No.
Figure 1.1 Greenhouse effect caused by greenhouse gases including CO ₂ resulting in the elevation of temperature in the environment [5].....	2
Figure 1.2 Graphical representation of U.S greenhouse emissions with major contribution by CO ₂ emissions [5].....	3
Figure 1.3 Process of CO ₂ generation, capture, transportation and storage [9] ..	4
Figure 1.4 Schematic of pre-combustion technology for efficient CO ₂ storage [12] .	5
Figure 1.5 Schematic of post-combustion technology for efficient CO ₂ storage [12]..	6
Figure 1.6 Post combustion CO ₂ storage technology by using calcium process [16]...	7
Figure 1.7 Oxy-flame combustion technology for CO ₂ storage [12]..	8
Figure 1.8 CO ₂ separation through various processes and substrates [23] .	10
Figure 1.9 Metal organic frameworks (MOFs) development by combination of metal source and organic linker [27] .	11
Figure 1.10 Characteristics of MOFs as selection criteria for CO ₂ sequestration and storage substrate ..	12
Figure 1.11 Percentage comparison of different synthesis methods for the production of MOFs [39] ..	18
Figure 1.12 The mechanistic representation of MOFs structure as a substrate for gas sensing ability [42].....	20
Figure 1.13 MOFs as a substrate for drug adsorption leading to drug delivery [45].....	21
Figure 1.14 MOFs as substrate for cancer treatment [47].....	22
Figure 1.15 MOFs doped with magnetic nanoparticles for the development of Magnetic Material [49] ..	23
Figure 1.16 MOFs implemented as electrolyte for various electrochemical processes [50].....	24
Figure 3.1 Schematic illustration of working of scanning electron microscopy (SEM) [69] ..	34
Figure 3.2 Schematic diagram of working of x-ray diffraction spectroscopy [70]...	35
Figure 3.3 Schematic illustration of working of fourier transform infrared (FTIR) spectroscopy [71] ..	36
Figure 3.4 Working principle of Thermogravimetric Analysis [72].....	37
Figure 3.5 Working principle of Brauner-Emmett-Teller (BET) [73] ..	38
Figure 3.6 Working principle of gas sequestration system [74] ..	39
Figure 5.1 XRD pattern of Zn-BDC and HMTA modified Zn-BDC MOFs	43

Figure 5.2	XRD pattern of Ni-BDC and HMTA modified Ni-BDC MOFs	43
Figure 5.3	SEM images representing the morphology of Ni-BDC.....	44
Figure 5.4	SEM images representing the morphology of Ni-BDC-HMTA.....	45
Figure 5.5	FTIR Spectrum of Zn-BDC and HMTA modified Zn-BDC representing all the bands corresponding to different metallic and non-metallic bonds available in the structure.....	46
Figure 5.6	FTIR Spectrum of Ni-BDC and HMTA modified Ni-BDC representing all the bands corresponding to different metallic and non-metallic bonds available in the structure.....	48
Figure 5.7	TGA profile of Zn-BDC and HMTA modified Zn-BDC representing mass loss trend with increasing temperature.....	50
Figure 5.8	TGA profile of Ni-BDC and HMTA modified Ni-BDC representing mass loss trend with increasing temperature.....	51
Figure 5.9	N ₂ absorption and desorption isotherms for Zn BDC \supset HMTA MOFs....	52
Figure 5.10	Pore size distribution of Zn-BDC \supset HMTA MOFs	53
Figure 5.11	N ₂ adsorption and desorption isotherms for Ni-BDC MOFs.....	54
Figure 5.12	Pore size distribution of Ni-BDC MOFs	54
Figure 5.13	N ₂ adsorption and desorption isotherm of Ni-BDC \supset HMTA MOFs.....	55
Figure 5.14	Pore size distribution of Ni-BDC \supset HMTA MOFs	55
Figure 5.15	XPS survey scan of Zn-BDC-HMTA MOF representing all the necessary identifying peaks	56
Figure 5.16	XPS B.E plot of (a) Zn 2p and (b) N 1s in Zn-BDC-HMTA MOF.....	57
Figure 5.17	XPS B.E plot of (a) O 1s and (b) C 1s in Zn-BDC-HMTA MOF.....	57
Figure 5.18	CO ₂ isotherms of Zn-BDC and Zn-BDC \supset HMTA at 283 K and 293 K.	58
Figure 5.19	CO ₂ isotherms of Ni-BDC and Ni-BDC \supset HMTA at 283 K and 293 K.	59

LIST OF SYMBOLS, ABBREVIATIONS AND ACRONMS

2D	Two-Dimensional
3D	Three-Dimensional
AAS	Atomic Absorption Spectroscopy
AES	Atomic Emission Spectroscopy
BDC	Benzene Dicarboxylate
BET	Braunauer-Emmett-Teller
BSE	Back Scattered Electrons
BTC	Benzene Tricarboxylate
C	Carbon
DABCO	Diazabicyclo octane
DMF	Dimethyl Formamide
EDX	Electron Dispersive X-ray
EIA	Energy Information Administration
FTIR	Fourier Transform Infrared Spectroscopy
GHG	Green House Gases
GWP	Global Warming Potential
HER	Hydrogen Evolution Reaction

HMTA	Hexamethylenetetramine
HOR	Hydrogen Oxidation Reaction
ICP	Inductively Coupled Plasma
IPCC	Intergovernmental Panel on Climate Change
IR	Infrared
MOF	Metal Organic Framework
OER	Oxygen Evolution Reaction
OMS	Open Metal Sites
ORR	Oxygen Reduction Reaction
PXRD	Powder Xray Diffraction
SEI	Solid Electrolyte Interphase
SEM	Scanning Electron Microscopy
TGA	Thermogravimetric Analysis
THF	Tetrahydrofuran
XRD	X-ray Diffraction

ABSTRACT

This study demonstrates that the synthesis of HMTA-modified Zn BDC and Ni BDC metal-organic frameworks leads to materials exhibiting superior structural properties and increased capacities for CO₂ adsorption. The integration of HMTA enhances the surface area and markedly improves the efficiency of these metal-organic frameworks (MOFs) in CO₂ capture, thereby establishing them as viable options for gas separation and environmental remediation applications. The Zn BDC and Ni BDC metal-organic frameworks (MOFs), along with their corresponding HMTA-modified variants, Zn BDC⊃HMTA and Ni BDC⊃HMTA are prepared through hydrothermal method. The synthesized metal-organic frameworks (MOFs) were characterized through a range of analytical techniques, which encompassed X-ray diffraction (XRD), scanning electron microscopy (SEM), Fourier transform infrared spectroscopy (FTIR), thermo-gravimetric analysis (TGA), and Brunauer-Emmett-Teller (BET) analysis. The XRD and SEM analysis demonstrated a crystal structure with notable morphological variations, suggesting that the inclusion of HMTA transformed the structure from irregular microspheres to interconnected sheets. The BET analysis revealed that the surface areas for Zn BDC⊃HMTA and Ni BDC⊃HMTA were significantly enhanced, measuring 66.53 m²/g and 220.91 m²/g, respectively, in comparison to their non-HMTA counterparts. The evaluation of CO₂ adsorption capacities measured by utilizing a high-pressure gas sorption analyzer demonstrated that the HMTA-modified MOFs displayed enhanced CO₂ adsorption properties, with Zn BDC⊃HMTA reaching a peak adsorption capacity of 3.50 mmol/g at 283 K, whereas Ni BDC⊃HMTA exhibited an adsorption capacity of 2.85

mmol/g. Both the values are higher than the unmodified BDC based MOFs. The results underscore the efficacy of HMTA as a modifying linker, significantly improving both the surface area and the adsorption capabilities of the metal-organic frameworks (MOFs).

Keywords: Metal organic frameworks, Organic Linker, Hexamethylene Tetraamine, CO₂ Adsorption, CO₂ storage.

CHAPTER 1: INTRODUCTION

The rising energy consumption has been reported in an Energy Information Administration (EIA) predicate. According to that report energy consumption will rise 57% in 2030 [1]. This percentage increases directly as the consumption of the available fuel increases for the increasing energy demand. Due to the increase in the consumption of the available fuel, greenhouse gases are also increasing considerably. During a year about 72% of the total greenhouse gasses emitted into the atmosphere during a year contains CO₂ gas [2]. This increase in CO₂ causes an increase in sea level which causes the increase in floods, climate change, global warming, rise in global temperature and the species extinct. The primary source of CO₂ emission is the use of combustion systems comprising fossil fuels. The use of coal fired power plants, and the burning of fossil fuels include coal, oil and natural gas into the industrial sector and the transport systems are the leading cause of the increase in CO₂ emission. The use of coal based power plants are also the major cause of the production of the CO₂ [3]. It is accepted that due to the increase in energy demand linked with the increase in world population and the development of the industrial sector, and the excessive use of fossils fuels. The concentration of CO₂ is also increased in our atmosphere and causes an increase in global warming.

1.1 CO₂ as Greenhouse Gas

The CO₂ molecules are also known as greenhouse gas. Greenhouse active gases are those gas molecules that have some dipole movement and IR active substances. So for example, the CO₂ is an IR active gas, when the IR radiation coming from the sun enters the earth atmosphere the CO₂ absorbs those IR radiations and their molecule starts vibrating due to dipole movement, the vibrating molecules emit radiation and those radiation. Other IR active molecules and the IR radiation then absorbed those radiations and the IR radiations was reminded in earth's atmosphere and did not reflect earth atmosphere and the absorb IR radiation causes the change in the climate conditions of the earth and the earth atmosphere On the other hand, the gasses like N₂ and O₂ present in

earth atmosphere are IR inactive molecules, and they have zero dipole movement and do not absorb IR radiation and reflect the IR radiation. This proved that CO₂ is an active IR molecule, and they absorbed IR radiation coming from the sun. As these radiations are not reflected instead they absorb by CO₂ molecules, Due to absorption the earth's temperature increases and the greenhouse effect increases [4]. The increase in CO₂ in the atmosphere causes an increase in the greenhouse effect, the greenhouse effect causes an increase in the earth temperature due to which the climate gets hotter and hotter day by day which results in the melting of the snow caps which cause floods. The increase in greenhouse gases can also cause an increase in the smog. Fig 1 shows the greenhouse effect.

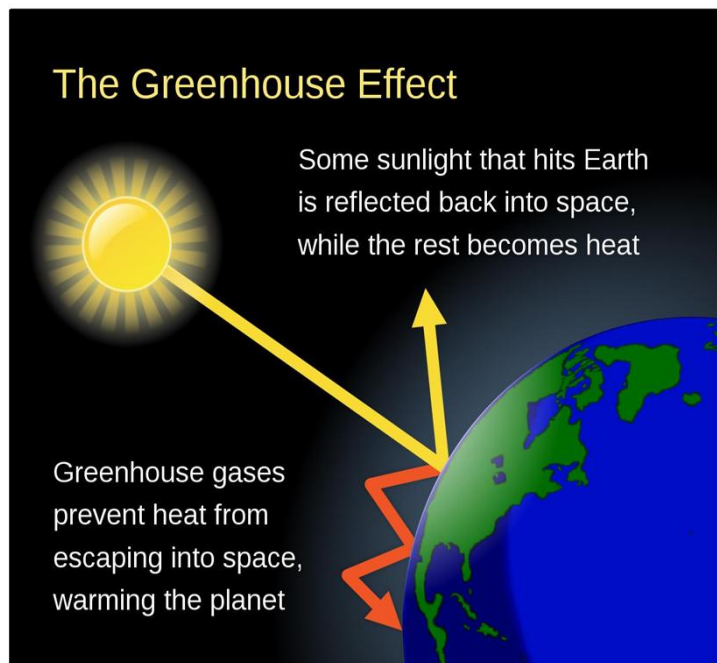


Figure 1.1: Greenhouse effect caused by greenhouse gases including CO₂ resulting in the elevation of temperature in the environment [5]

1.2 Role of CO₂ in Global Warming

Carbon dioxide has been considered the most important for two main reasons. Firstly, CO₂ has been proved to have caused most of the warming (Fig. 1.2) since 1750 as compared to other climate drivers by Intergovernmental Panel on Climate Change (IPCC)

in a “global climate assessment report” in 2013 [6]. The IPCC estimated the “radiative forcing” (RF) of each climate driver, that is the net rise (or decline) in the quantity of energy getting to the Earth’s surface credited to that climate driver. Positive and negative RF values stand for average surface warming and cooling respectively. In the result, CO₂ has the maximum positive among all the anthropogenic climate drivers calculated by IPCC [7]. Secondly, CO₂ resides in the atmosphere for a longer time than any other GHG. Although Global Warming Potential (GWP) i.e., how much heat a GHG fences in atmosphere up to specific time horizon, of CO₂ is low as compared to other greenhouse gases but it has longer lifetime causing larger greenhouse impact [8].

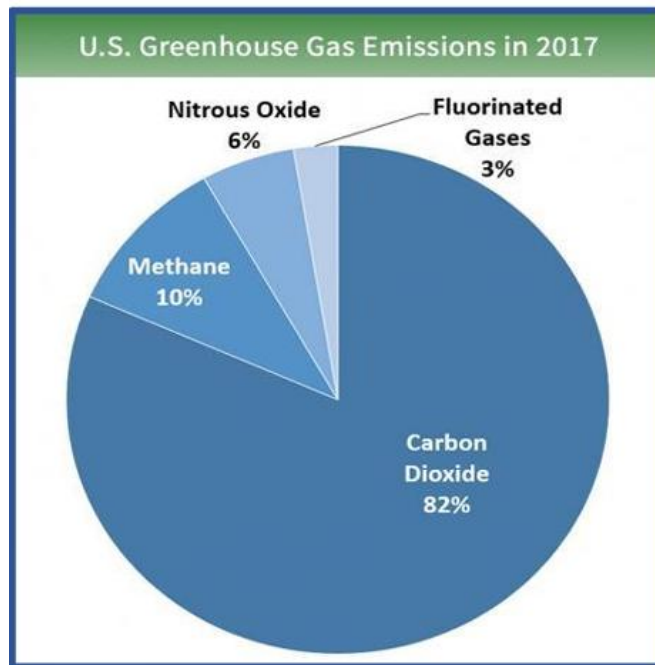


Figure 1.2: Graphical representation of U.S greenhouse emissions with major contribution by CO₂ emissions [5]

1.3 Carbon Capture & Storage

As energy demand increases, the consumption of fossil fuels also increases. There is an urgent requirement to reduce the emission of CO₂ from the industrial process to minimize the effect of CO₂ on climate changes. To reduce the emission of CO₂ Carbon

Capture Storage, methods are used. Many of the carbon capture technologies are now commercializing to reduce CO₂. Their primary aim is to capture CO₂ from large-scale power plants, industrial processes and transportation. Carbon Capture Utilization or Storage (CCUS) is a process that can capture carbon and utilize the captured carbon for the synthesis of valuable products. The CCUS techniques are not only for the capturing of CO₂ gas, but it can also work how to use the captured CO₂ to produce other materials.

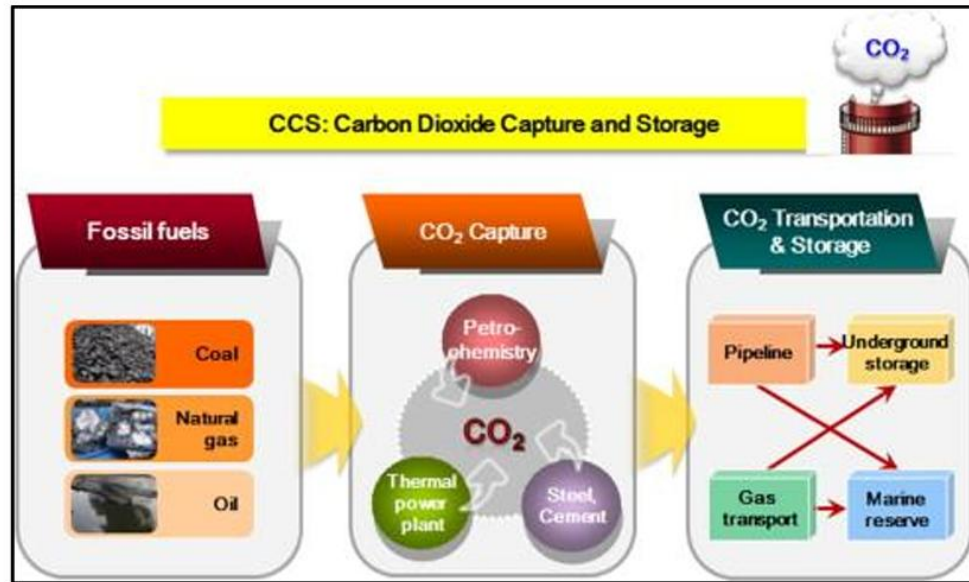


Figure 1.3: Process of CO₂ generation, capture, transportation and storage [9]

The Carbon Capture Storage and Utilization consists of four steps which includes: The first step is the capturing of the CO₂ gas from the emission sources, the treatment of captured CO₂, transportation of the treated CO₂ gas to the storage sites and then the storage of CO₂ and then the stored CO₂ is further used for the production of the different chemicals as it the raw material for various processes like in urea production the CO₂ is used as a raw material. There are four leading conventional Carbon Capture Storage technologies that are mostly used in the industrial sector.

Following are the leading conventional technologies [10]

- Pre-combustion technology

- Post-combustion technology
- Oxy-flame technology

1.3.1 Pre-Combustion Technology

The pre-combustion technology is one of the most used technologies. The pre combustion carbon capture technology involves the reaction between the fuel and the oxygen (which is obtained from the air through an air separation unit), This reaction mainly gives us the product called synthesis gas (syn gas). The syn gas is a mixture of carbon monoxide and hydrogen. Later, the carbon monoxide from the syn gas is converted into CO₂ and H₂, by reacting to a CO with steam in a catalytic converter this reaction is mainly known as shift reaction in which the CO is further converted into the CO₂. After that the CO₂ is separated by physical and chemical processes resulting in hydron rich fuel gas. The CO₂ is stored and used as a raw material in many other chemical processes [11]. Fig 1.4 shows the schematic of pre combustion technology.

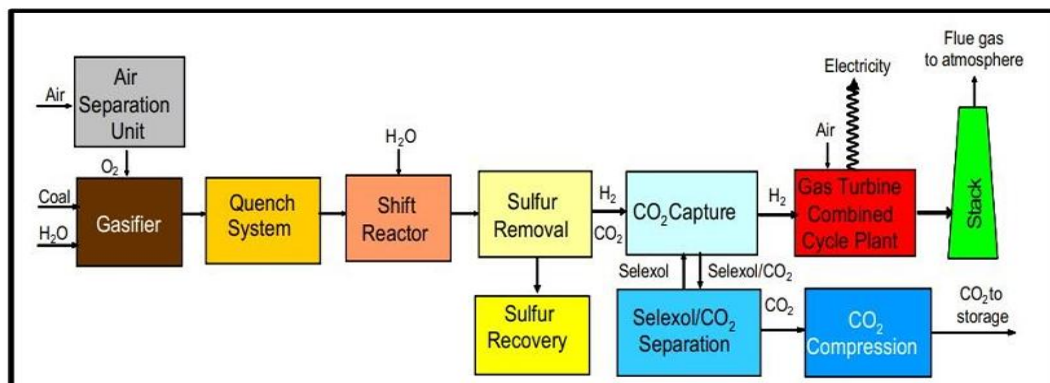


Figure1.4: Schematic of pre-combustion technology for efficient CO₂ storage [12]

This technology is still not mature enough to be implemented in to the industrial level because of the highest capital investment cost, this technology requires a lot of work to be implemented in the industrial sector.

1.3.2 Post-Combustion Technology

In post-combustion technology CO₂ is separated from the flue gasses after the combustion of fossil fuels, The CO₂ is captured using adsorption, absorption and membrane separation. It is the only technology that can be retrofitted to existing plants. The biggest problem with this technology is the separation of CO₂ from the flue gasses as the flue gasses contain a large amount of nitrogen N₂ [13]. Post combustion technology is done by using calcium processes by using alkali earth metal based solid adsorbents. The calcium process is the most used example of post combustion.

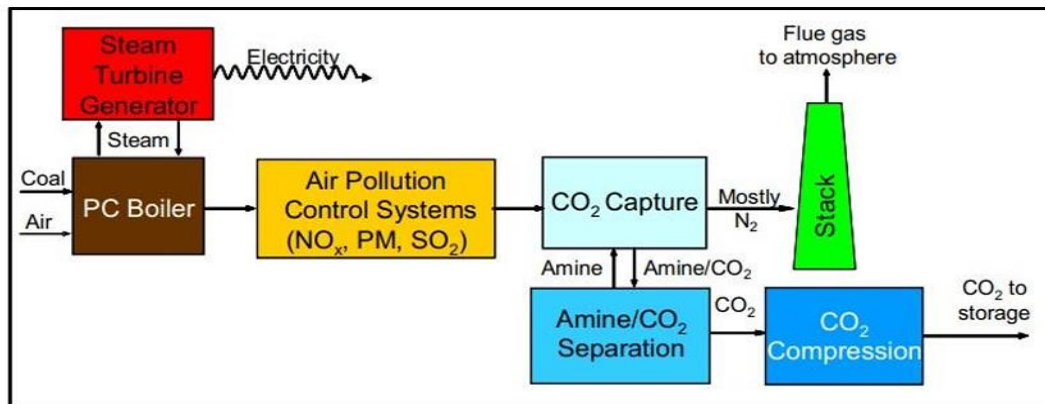


Figure 1.5: Schematic of post-combustion technology for efficient CO₂ storage [12]

Currently, solid absorbents based on alkaline earth metals are being utilized to capture CO₂ from flue gases. Research has also focused on these sorbents for CO₂ capture at elevated temperatures in the absence of water vapor. For instance, calcium oxide (CaO), an alkaline earth metal, can undergo a reversible reaction with CO₂ to produce calcium carbonate (CaCO₃), making it suitable for both pre-combustion and post-combustion carbon capture applications [14]. As illustrated in Fig 1.5, the process involves a vessel known as the carbonator, where the carbonation reaction occurs. In the carbonator, CO₂ reacts with solid CaO, resulting in the formation of CaCO₃, while nitrogen (N₂) and any excess CO₂ are expelled from the flue gas at approximately 600 °C. The produced CaCO₃ is then transferred to a second vessel, referred to as the calciner. In the calciner, CaCO₃ is subjected to heating at temperatures ranging from 900 °C to 950 °C, which drives the

reverse reaction, releasing CO₂ that can be used to regenerate the CaO sorbent, which is subsequently returned to the carbonator.

The carbonation reaction is highly exothermic, aligning well with the temperature requirements of a steam cycle, thus allowing for heat recovery. Studies have investigated the decomposition conditions of CaCO₃ particles for CO₂ capture in a steam-diluted atmosphere within a fluidized bed reactor. Results indicated that increasing the steam dilution percentage in the CO₂ supply gas enhanced the decomposition conversion of limestone. However, the reactivity of the natural limestone-derived sorbent (CaO) tends to diminish over multiple CO₂ reaction cycles due to morphological changes such as pore shape alterations, pore shrinkage, and grain growth during heating. To mitigate the degradation of sorbent morphology caused by sintering and to produce more robust sorbent particles that resist attrition, further advancements are necessary [15].

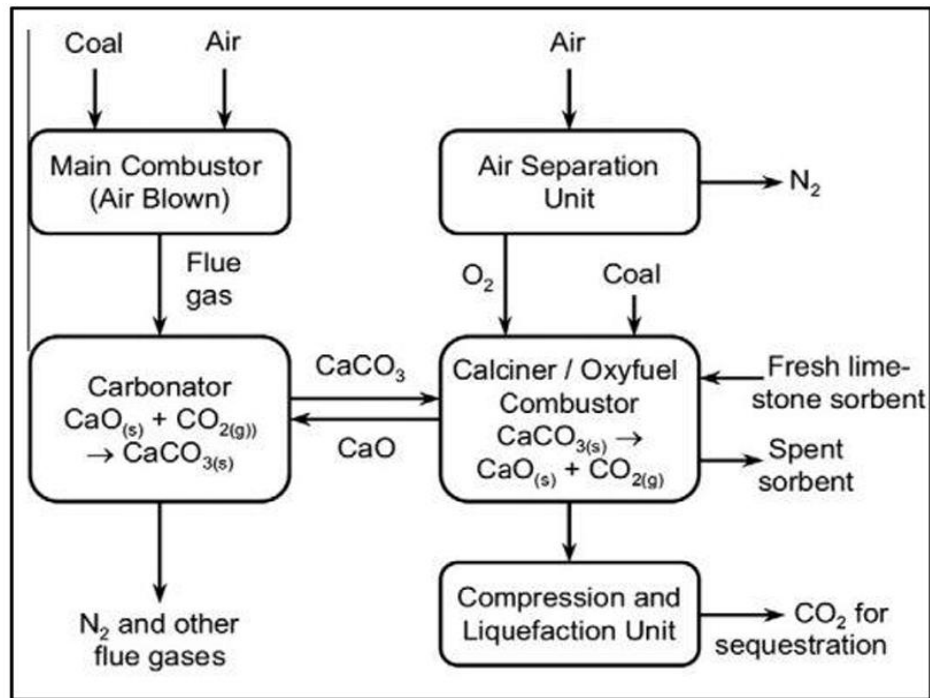


Figure 1.6: Post combustion CO₂ storage technology by using calcium process [16]

1.3.3 Oxy-Flame Combustion Technology

Oxy- flame carbon capture technology is one the leading technologies now a days for the capturing of CO₂. This involves the burning of fossils fuels in the presence of pure oxygen instead of air. This can be done to increase the concentration of CO₂ in the flue gasses later the CO₂ can be separated from the flue gases. The flue gasses contain CO₂ and water. CO₂ can be separated by the process of dehydration and low by using temperature purification process. It is superior to post combustion carbon capture technology because it cannot contain N₂ in the flue gasses like post combustion technology, oxy flame only contains CO₂ and water, and it is free from nitrogen and its purification is easier. This methods give us the highest recovery of CO₂ and also give concentrated CO₂ with no N₂ present in the gas stream [17].

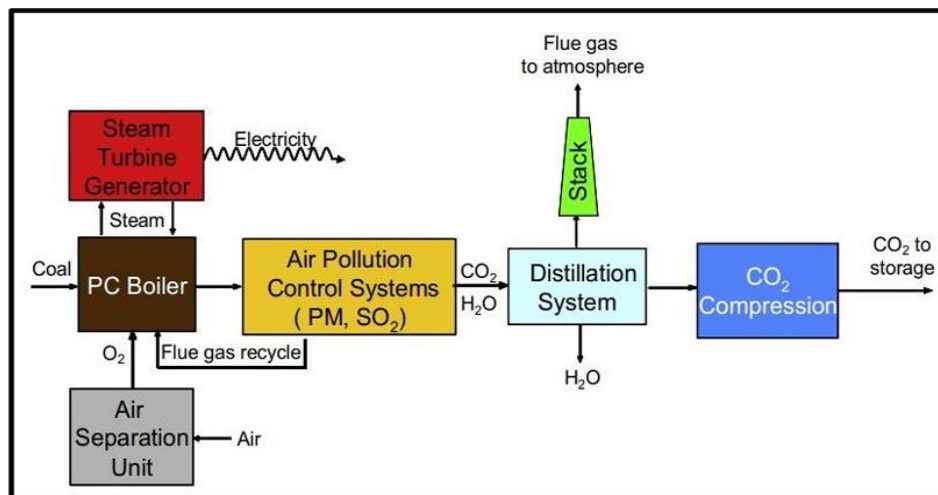


Figure 1.7: Oxy-flame combustion technology for CO₂ storage [12]

1.4 CO₂ Capture by Absorbents

Currently Carbon capture using adsorbents technology is the most advanced technology. There are many types of adsorbents that are used for the capturing of CO₂. The adsorbents are the most used technology because the adsorbents contain a high surface area, low cost, thermal stability and high adsorption rate of CO₂. Many types of

adsorbents are used including alkali earth metal, zeolite, carbon-based, silica-based adsorbents and metal organic framework adsorbents. Carbon-based adsorbents are thermally stable, and these adsorbents require less energy for the regeneration process.

However, the only problem with carbon-based adsorbents is less adsorption capacity, low surface area and pore size. The zeolite adsorbents show suitable adsorbent quality and have good structure and pore size. However, the limitations with zeolite adsorbents are that their adsorption decreases as the temperature increases. These adsorbents are highly hydrophilic in nature. Minute moisture can be inactive in the zeolite adsorbents. Nowadays the alkali earth metal based solid adsorbents are also used to capture CO₂ from the flue gas. At high temperatures in the absence of water vapor sorbents for CO₂ capture from flue gas have also been investigated. The alkali earth metals is used in calcium based post combustion processes to produce concentrated stream of the CO₂. Alkali earth metal, such as CaO can reversibly react with CO₂ to form alkali earth metal carbonate CaCO₃ which is used in processes like pre-combustion and post-combustion carbon capture applications [18, 19].

Metal-organic frameworks (MOFs) are increasingly favored as adsorbents due to their distinctive properties when compared to other materials. These advantages include rapid adsorption rates, substantial surface areas, large pore sizes and volumes, strong affinity for CO₂, cost-effectiveness, and minimal energy requirements for regeneration. Consequently, selecting the right adsorbent is crucial for effective carbon dioxide adsorption. Several factors should be considered prior to the selection of an appropriate adsorbent [20, 21]. The parameter is responsible for the structure, quality and the properties of the adsorbents. The parameters include adsorption and desorption kinetics, operating condition, temperature and pressure conditions, pH of the adsorbents, temperature and moisture of the surrounding, these parameter are responsible for the capturing capacity of the adsorbent, mechanical and chemical stability and the high CO₂ selectivity [22].

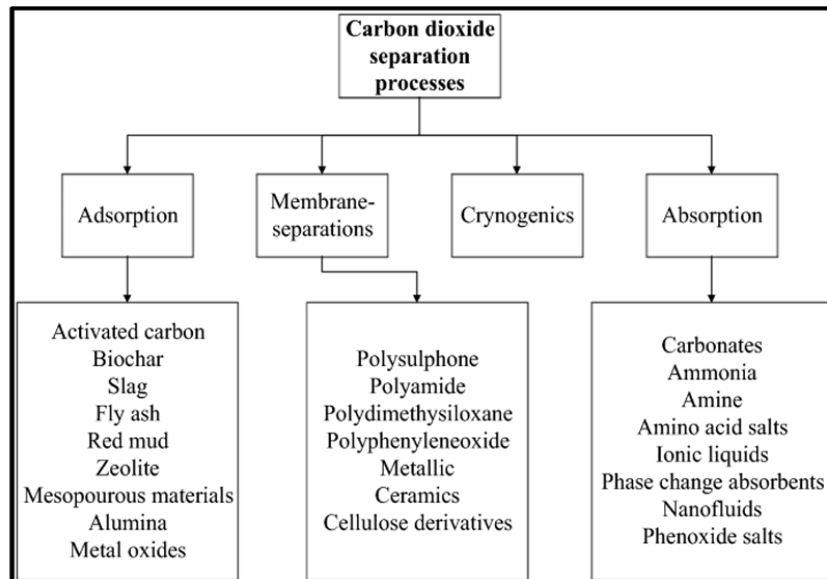


Figure 1.8: CO₂ separation through various processes and substrates [23]

1.4.1 Metal Organic Frameworks (MOFs) for CO₂ Capture

Metal Organic framework provides an excellent opportunity to develop an adsorbent that can fulfill the criteria for suitable sorbent. MOFs have benefit over other adsorbents because of its unique properties like high surface area, stability, channels, permanent porosity and functionalizability of organic linkers for carbon capture. Yaghi et al. were the first to report MOFs for CO₂ capture at room temperature with stable porosity after removing the guest ions [24] following which many new MOFs were developed for CO₂ capture. For MOFs to have high performance there are a few parameters of concern. First of all, it's important for MOFs to have high selectivity for CO₂ [25] over other impurities present in flue gases since low partial pressure of CO₂. Another important parameter that decides the energy penalty of carbon capture is the affinity of MOFs towards CO₂. If the affinity is high this will lead to high energy requirement for desorption (regeneration) while on the other hand if the affinity is low, it will lead to low CO₂ selectivity of MOFs [26]. Lastly, for commercial application of MOFs it is important that the MOF is stable under adsorption and desorption cycles to be used for long periods of time. Also, the uptake density must be high so that adsorbent bed should be minimized

[49]. MOFs materials can be further optimized to synthesize adsorbents appropriate to meet the above-mentioned performance criteria.

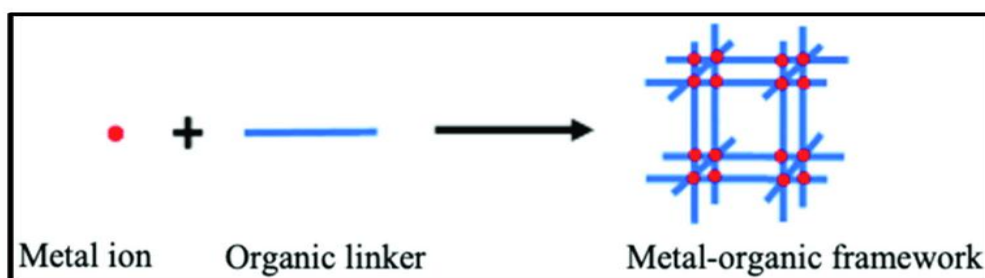


Figure 1.9: Metal organic frameworks (MOFs) development by combination of metal source and organic linker [27]

1.5 MOFs Selection Criteria

The selection of MOF is one of the most important and major steps, the MOFs should be selected according to the applications for which MOFs are used. The MOFs used for the adsorption of CO₂ must fulfil the following criteria

- The MOFs should have a high surface area, and high adsorption capacity. The Adsorption capacity of MOFs is determined by the pressure/temperature isotherms [28].
- The MOFs should be highly selective towards CO₂ while the selectivity in terms of adsorption should be defined as the ratio of CO₂ to the other gaseous components such as oxygen, methane, nitrogen etc. [20]
- The MOFs must possess a high and fast rate of adsorption, It also shows desorption that is higher than the rate of adsorption [29].
- The stability determines the lifeline of MOFs, It determines that after how much time the MOFs should be replaced. By considering this factor the strength of MOFs should be higher [30].
- The MOFs should be at a low cost, green in nature, it does not affect the environment.
- The MOFs should have good chemical and mechanical stability [21].

Choosing MOFs for the use of CO₂ is based on many screening factors. These factors include the selectivity that how much the MOFs is selective towards the CO₂, ease of synthesis is a major factor as it belongs to the cost, the MOFs show high affinity towards the CO₂ so that the more adsorption occurs, MOFs is hydrophobic in nature so that the atmosphere moisture will not harm the MOFs, the morphology is also crucial because it includes surface area, pore size, pore volume and the most important part of the screening of the MOFs is regenerate ability MOFs should only use whose regenerate ability is very excellent.

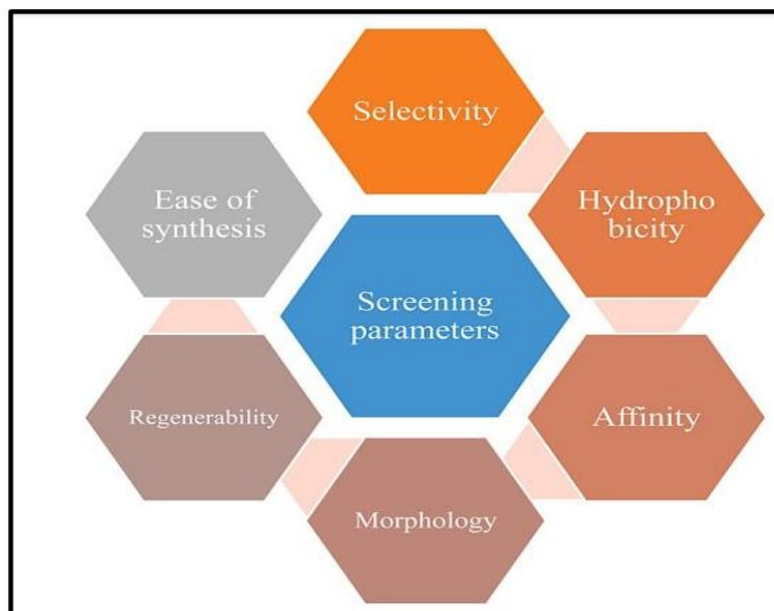


Figure 1.10: Characteristics of MOFs as selection criteria for CO₂ sequestration and storage substrate

1.6 Methods for Synthesis of MOFs

Various methods are used to the synthesis of MOFs, these methods include solvo/hydrothermal method, microwave synthesis method, electrochemical method, sonochemical method, spray drying method and flow chemical methods. Every method has its own advantages and disadvantages. These methods are produce MOFs which are

of different morphologies and the MOFs that are produced from various methods are used in different applications [31]. The various methods for the synthesis of MOFs are described below in detail.

1.6.1 Solvothermal or Hydrothermal Method

Solvothermal is the most common method used for synthesizing MOFs. This is the most widely used method for the preparation of the different types of MOFs which are used in different applications. This method is based on the principle of the heating of the reagents dissolved in the universal solvents in a tightly closed autoclave reactor and then heated that reactor for about some time according to the MOFs are producing. In this method the metal and organic linkers are dissolved in a solvent and after mixing well the homogenous solution is poured into Teflon lined autoclave and put that autoclave into hydrothermal reactor at a temperature of 373 K for about 24 hours. The size of the crystal in this method depends upon the pressure that is built up in the reactor and the temperature given to the reactor. Usually, a more significant crystals yield is obtained when the pressure built up inside the reactor is high and is subjected to a longer duration. After the preparation of crystals, the crystals are washed with the solvents. Usually, the solvents that are used in washing are water and ethanol. After washing the crystals are dried in a vacuum oven for about 24 hours. The usually used solvothermal solvents are ethanol and N, N-Dimethylformamide (DMF). The temperature range in the solvothermal process is from 350K to 470K and the time duration is about 1-2 days [32].

Some major advantages of this method are;

- The MOFs that are prepared by this method have excellent crystal size.
- This method produces large quantity of MOFs, this method is high yield.
- The MOFs made by solvo/hydrothermal method contains high surface area, pore size and the MOF prepared by this method has good structure.

However, it has some disadvantages as well;

- The main disadvantage of this method is that this method takes a very long time.
- This method is an expensive method because the solvents that are used are expensive.

1.6.2 Microwave Synthesis Method

The microwave synthesis method is based on microwave radiation. In this method the reactants are placed into the tightly closed system, after that the system is subjected to the intense microwave radiation. The microwave radiation has provided the necessary conditions that fulfill the requirements for the formation of MOFs crystals. This method is popular because it is the fastest method for the synthesis of MOFs crystals. This method takes only a few hours to complete the reaction. The temperature range is 303K-393K for this method. For example, the synthesis of MOFs and zeolites imply the same techniques. The synthesis done via microwave-assisted technique relies upon the interaction between mobile electric charges and electromagnetic waves. These could be electron/ion in a solid or molecules/ion in a solution. In solids, the electric current is generated, and electric resistance of solids causes heat. While in a solution, electromagnetic field is formed which aligns polar molecules in an oscillating manner so that orientation of molecules is changed permanently. Therefore, by applying appropriate microwave frequency, vibrations between molecules occur, which causes collision and leads to higher kinetic energy such as temperature or the system internal energy. Direct interaction of microwave radiation with solutions applies an energy efficient way of increasing kinetic energy. This leads to homogeneous heating and high heating rates throughout the system [33].

Some major advantages of this method are:

- The advantage of this method is that the crystals are excellent size
- Another advantage of this method is that this method is usually the fast method as compare the solvo/hydrothermal method.

However, it has some disadvantages as well.

- The main disadvantage of this method is that this method gives the low yield
- The other advantage of this method is that this method is difficult to scale up

1.6.3 Electrochemical Method

The electrochemical method involves the use of electricity in the synthesis of MOFs. This method is the fastest method for the synthesis of MOFs. It requires only a few minutes for the synthesis of MOFs. In this method, we use metal ions instead of metal salts. The only problem with this method is that the crystals are produced from low surface area and poor quality crystals [34].

Some major advantages of this method are;

- The main advantage of this method is that this method is one of the rapid methods as compared to other methods, this method takes mins for the synthesis

However, it has some disadvantages as well;

- The crystals produced from this method are very low quality and are poor size
- The crystals produced from this have low surface area, low pore size, low pore volume and they are of very poor quality.
- Another disadvantage of this method is that this is the most-costly method, as electricity is needed in this process, which makes it costly

1.6.4 Sonochemical Method

The sonochemical method involves sound frequencies for the completion of the reaction, and it facilitates crystal formation. In this method first the reagents are taken in a beaker and then the beaker containing is subjected to the sound waves having high frequencies. After the reaction the crystals are filtered out and then dried in vacuum oven [35].

Some major advantages of this method are;

- The production time of this method is very fast, this method requires very little time for production.

However, it has some disadvantages as well.

- This method gives the very less amount of product, the yield is of this method is very low.

1.6.5 Spray Drying/Evaporation Method

In this method there is no external force required compared to the other methods. It is the most straight forward method for synthesizing MOFs, in this method the solvent gets evaporated by natural evaporation after natural evaporation the crystals are formed, but the problem with this method is that this method is a much time consuming method and the yield that is obtained from this method is also very low these reasons does not allow this method to be suitable for the use in industrial sector, as it is non convenient method [36].

Some major advantages of this method are;

- This process does not require any external force, the cost of this method is very low. This method is one of the cheapest methods among other methods
- This method is one of the simplest methods as it does not require external process

However, it has some disadvantages as well.

- The disadvantage of this method is that this method is a very time-consuming method, this method takes much time to synthesize the MOF.
- The other major disadvantage of this method is that this has a very low yield.

1.6.6 Chemical Flow Method

The chemical flow synthesis method is another type in which there no external force is required to complete the reaction. In this method the reactants are left to complete the reaction no external force is applied. The average time is from 2 min to 6 days and the temperature required is 303K-573K [37].

Some major advantages of this method are;

- The main advantage of this method is that this method requires very little amount of energy as the reactions are their own.
- This method gives a higher yield as compared to the spray drying method
- This method does not require any external force, which make the process less expensive and this method is cheaper one as compared to other methods

However, it has some disadvantages as well.

- The major disadvantage of this method is that it is time consuming method

1.6.7 Comparison of Different Synthesis Methodologies

Figure 1.11 shows the usage percentage of the different synthesis methods that are used to produce MOFs. The graph shows which method is more widely used and which one is the least used method. In this graph the usage percentage of the different methods are plot on y-axis, while the methods are plot on the x-axis of the graph and the bar graph has been obtained. The graph show that most used method is solvothermal method, as this method usage percentage is 70% because this method gives the higher quality crystals, high yield and the crystals obtained from this method are of good quality having higher surface area, the other most used method after the solvothermal method is hydrothermal method, the hydrothermal method usage is of approximately 15%, the other method that comes after hydrothermal method is the use of the microwave method the usage of this method is of 9%, the methods that are not used mostly are sonochemical and

mechanochemical methods, these methods are not widely used, their usage percentage is only 5%, the electrochemical method is one of the most least used method for the production of the MOFs, because this is the costly method as it required electricity and this method give the lower quality crystals and very less yield. The usage of this method is only 0.1%, This make can save the time, as it the fast method but the usage shows that this method is very negligible and it requires more attention to make this method suitable to use [38].

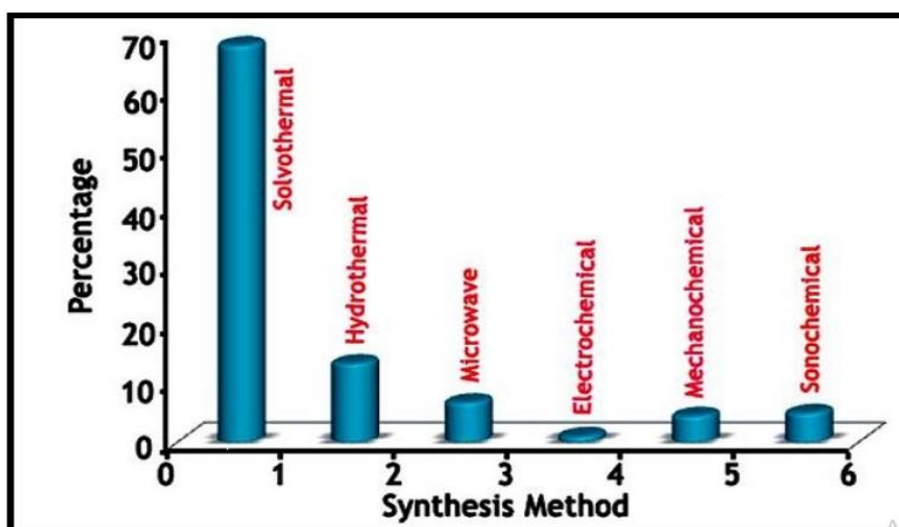


Figure 1.11: Percentage comparison of different synthesis methods for the production of MOFs [39]

1.7 Applications for MOFs

MOFs are used in various applications, MOFs do not rely on specific applications instead they can use in various applications, including MOFs as a sensor, MOFs for gas separation and storage, MOFs for drug delivery, MOFs can also be used as a catalyst in some chemical processes. MOFs as a gas separation and storage play an important role now a days, many of the MOFs are developed now for the separation and storage of the gases. Gases are a very beneficial source when it comes to energy production so for the effective storage of gases some good storage tanks are essential. Many options are available for this purpose, but some require multi-stage compressors, high pressure tanks

or are too expensive for practical use. Therefore, is a need of some alternative, reliable, cheaper storage devices. The most widely examined and used material is MOFs, which serves as an alternative for gas storage and separation purpose but also offers clean mobile energy. Convenient synthetic procedures, variable functionalization, adjustable pore size, high surface area are some of those properties of MOFs due to which they are superior to other porous materials. So, that is why these characteristics of MOFs show better efficiency and performance than the other available materials. MOFs has many applications but some of the common applications that are mostly used are listed as below, these listed applications are most used applications [38, 40].

- MOFs as a sensor
- MOFs for gas separation and storage
- MOFs for drug delivery
- MOFs for cancer theragnostic
- MOFs as a magnetic material
- MOFs for electrocatalysis

1.7.1 MOFs as a Sensor

The electrochemical sensor is one of the main constituents in analytical chemistry. Electrochemical sensors can provide us with high selectivity and sensitivity as compared to conventional techniques like atomic absorption spectroscopy (AAS), atomic emission spectroscopy (AES), inductively coupled plasma mass spectroscopy (ICP MS), and chromatography. Various MOFs based composites are now developed as efficient electrochemical based sensors in the field of chemistry, environmental and biochemical. MOFs sensors are widely used in analytical chemistry. The MOFs sensors can also be used for the detection of the heavy metal, organic compounds, gas sensing [41].

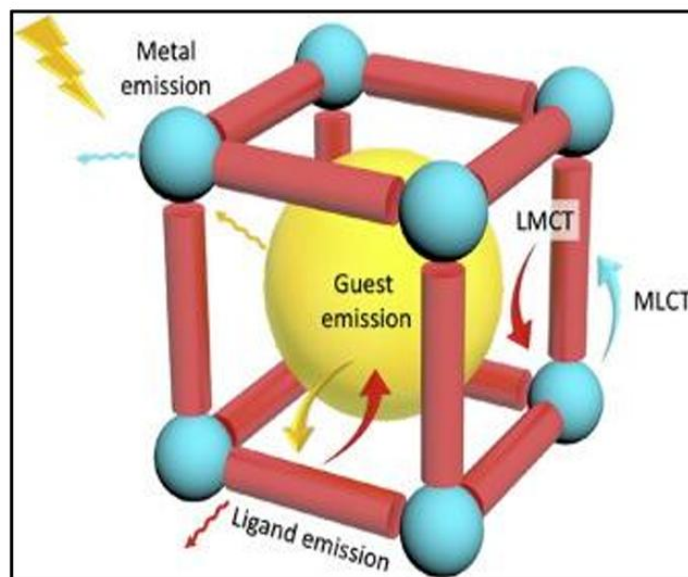


Figure 1.12: The mechanistic representation of MOFs structure as a substrate for gas sensing ability [42]

1.7.2 MOFs for Gas Separation and Storage

The MOFs have received great attention from gas separation and storage. Nowadays many MOFs and its composites are developed for gas separation and storage. For the better activity of MOFs in gas separation and storage the ligands and metals are chosen carefully, Also the functionalized group is an essential factor in the gas adsorption and storage. MOFs with their unique property like porosity, surface area, pore size and pore volume can adsorb the gases, and facilitate the gas separation. The MOFs promise to store some of the essential gases such as H_2 , CO_2 , CH_4 etc. The development of the various MOFs for gas separation has been witnessed during the last decade. Since its discovery in the 1990s, various MOFs have been synthesized by different gas separation and storage techniques. Therefore, incorporation of ligands or functionalizing organic groups for the appropriate functioning of MOFs should be chosen carefully. Another metal is incorporated via a new node for the appropriate functioning of MOFs. This is called bimetallic MOFs. It has dual properties of both the metals attached to same or different ligands. In general, of adding metal nodes in same framework will allow more metals to

incorporate with each other enhancing the defects in MOFs, increasing in its activity, porosity and synergistic effects between metal by integration, which can boost their intrinsic and transit properties [43].

1.7.3 MOFs for Drug Delivery

Drug delivery is one of the essential applications for the health of human care and also in biomedical. Due to its self-assembly of metal and organic linker at mild conditions MOFs provide us with several applications in the field of biomedical. MOFs as a drug carrier provides us with the following advantages as compared to other materials. Time to release the drug can be prolonged using amorphous MOFs from 2 to 30 days. It shows that the amorphous nature of MOFs is capable enough to catch the drug inside its cavities for proscribed drug delivery and to slow the release of drug molecules. Many factors affect the drug delivery applications of MOFs such as physiochemical characteristics, pore size and 3D arrangement which give versatility to the drug fitting in the cavities of MOFs. Nevertheless, drug delivery through MOFs is more effective than nanocarriers because the drug delivery takes place in a controlled manner and slowly in the case of the former by matrix degradation. At the same time later gives a burst effect on the release of the drug [44].

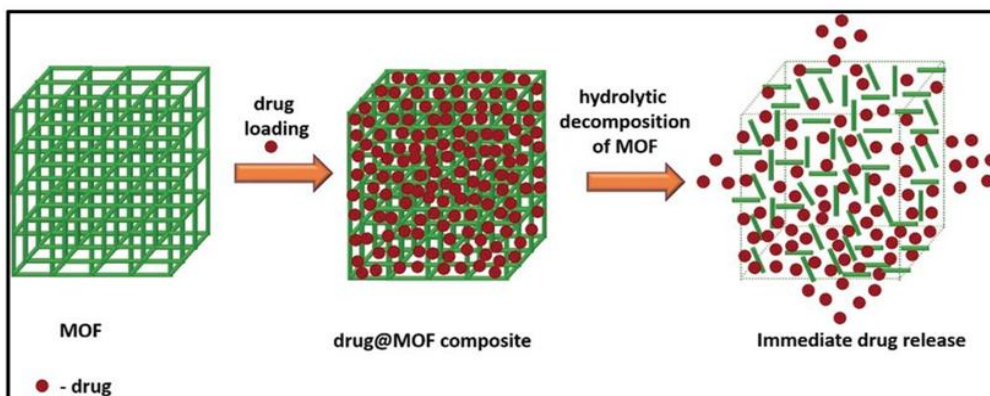


Figure 1.13: MOFs as a substrate for drug adsorption leading to drug delivery [45]

1.7.4 MOFs for Cancer Theragnostic

Many of the MOFs are now reported that are used for the treatment and the diagnosis of cancer cells. MOFs can also be used in many of the cancer treatments methods like MOFs can be used in Chemo and other treatments methods for the treatment of the cancer cells. MOFs have a capacity to be used in cancer treatment as it gives some positive results against cancer. MOFs as a cancer treatment has a very potential but the only problem is that it needs some work and attention. However, much of the work is needed to overcome the limitations of current treatment. For example MOFs after coating with polymer is used for the treatment of cancer [46].

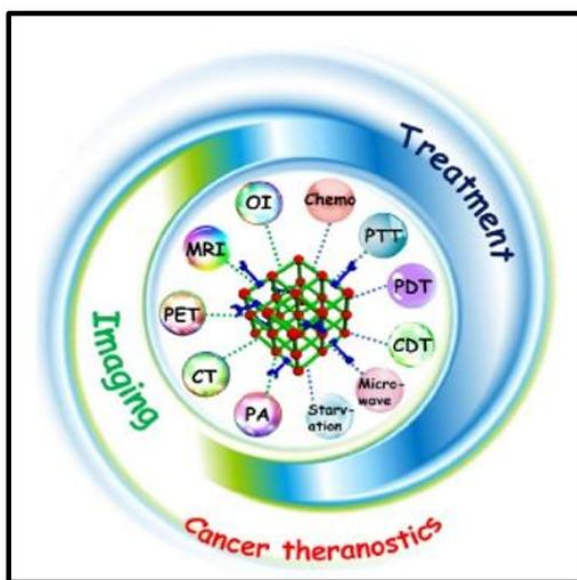


Figure 1.14: MOFs as substrate for cancer treatment [47]

1.7.5 MOFs as a Magnetic Material

MOFs from the last 30 years have been used to make revolutionary magnetic material. Many of the MOFs are prepared that are used as magnetic material but still there is a lot of work to do to make the MOFs as magnetic material. MOFs is also known as the porous coordination polymers. In such MOFs, its crystalline network faces a dynamic

change when exposed to external stimuli. Such materials are born with adjustable magnetic properties. Magnetic framework composites are the latest group of compound that meets magnetic character of metal with functional properties [48].

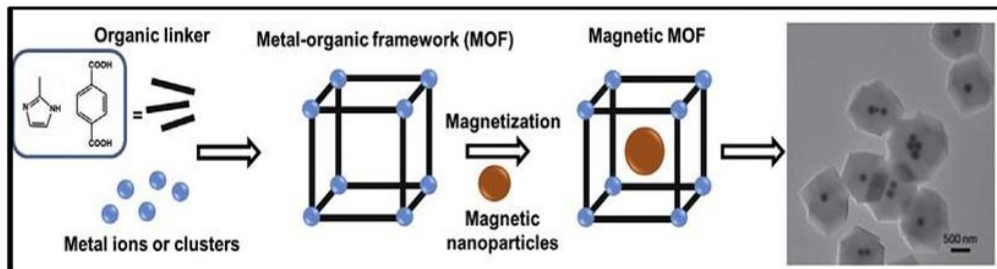


Figure 1.15: MOFs doped with magnetic nanoparticles for the development of Magnetic Material [49]

1.7.6 MOFs for Electrocatalysis

Catalysis is one of the main applications of metal-organic frameworks. Their large porosities recognize MOFs, diversified/tunable pore surfaces, uniform pore shape/size, redox properties and many other unique physical and chemical properties. Incorporating heterogeneous properties, MOFs can possess various acidic or basic sites for catalysis with coordination structure and surrounding environment, like the structure present in complexes of proteins and molecular metals. Combining the properties of molecular homogeneous and nonorganic heterogeneous catalysts, Metal Organic Frameworks can perform as a promising agent in achieving high catalytic mechanisms and performances.

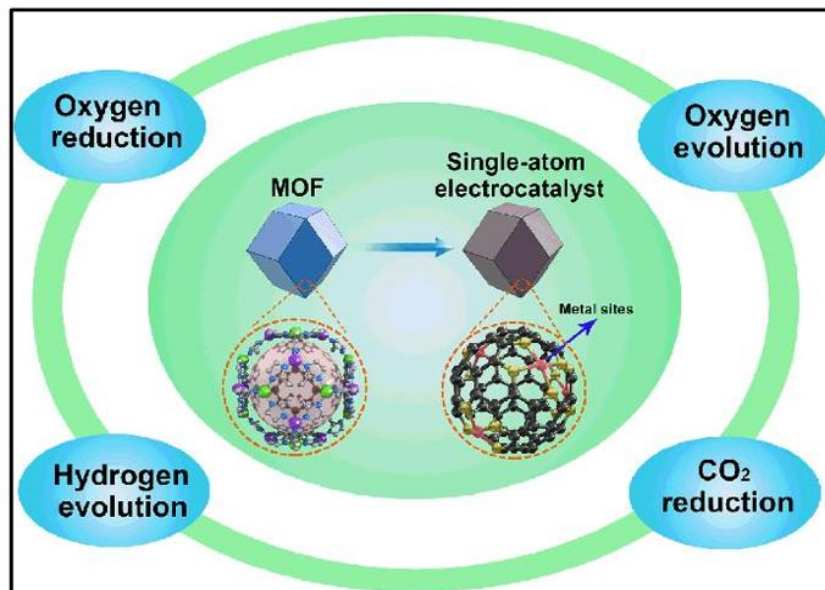


Figure 1.16: MOFs implemented as electrolyte for various electrochemical processes [50]

An Electrochemical reaction is one of the essential parts of chemical reaction. These chemical reactions proceed by the transfer of electrons directly between atoms, molecules or ions. They are often described as reduction-oxidation or redox reactions. Redox reactions can be separated into two half-reactions associated with the electrodes: the reduction process occurring at the cathode and the oxidation process taking place at the anode. As these reactions are directly connected to clean energy conversion and storage, they are found in electrochemical devices such as fuel cells, batteries, electrolytic cells, corrosion inhibitors and supercapacitors. The reactions performed in these cells involve different half-cell reactions such as, hydrogen oxidation reaction (HOR), oxygen reduction reaction (ORR), hydrogen evolution reaction (HER), oxygen evolution reaction (OER). MOFs incorporate large surface areas which reside in its porous structure. The crystallography technique can visualize the structure of MOFs for catalytic activity by. It is important to note that solid state and solution state structures of molecules differ from each other, creating MOFs which can be engineered according to the needs of environment. The primary issue with these structures in electrochemical reactions is their

low stability. Electrochemical reactions are usually performed under ionic solution or electrolyte (mainly based on water) with a high acidic or basic environment [51].

CHAPTER 2: LITERATURE REVIEW

The details of various MOFs structures consisting of a variety of metals and organic linkers is provided below.

2.1 DABCO based MOFs

Ijlal Aamer et al. [52] reported the synthesis of three-dimensional (3D) Zn-BDC-DABCO and Co-BDC-DABCO metal-organic frameworks (MOFs) was achieved through a solvothermal approach, with the primary application of capturing CO₂. By incorporating DABCO into the layered structure of the MOFs, a transition to a 3D configuration occurs, which significantly improves CO₂ adsorption capabilities. The CO₂ capture performance of these MOFs was evaluated at a temperature of 25 °C and under pressures ranging from 0 to 25 bars. The Zn-BDC-DABCO MOF demonstrated an adsorption capacity of 6.3 mmol/g, while the Co-BDC-DABCO MOF exhibited a capacity of 4.4 mmol/g. [52].

2.2 Amino Functionalized MOFs

Lin, Xiaoying, et al. [53] reported the synthesis of Mg-MOF-74, the amino-functionalized Mg-MOF-nNH₂. The addition of amino-containing ligands enhances CO₂ adsorption. Mg-MOF-nNH₂, featuring double ligands, was synthesized using magnesium as the central metal and incorporating 2,5-dihydroxyterephthalic acid alongside 2-amino terephthalic acid as ligands. The CO₂ saturation adsorption capacity for Mg-MOF-1/8NH₂ was measured at 3.9 mmol/g at 303 K. When compared to Mg-MOF-74, the CO₂ adsorption capacity of Mg-MOF-1/8NH₂ exhibited increases of 9%, 18%, and 44% at temperatures of 303 K, 313 K, and 323 K, respectively.

2.3 Benzene Tricarboxylate (BTC) based MOFs

Leena Aftab et al. [54] reported the synthesis of MOF used to capture CO₂. The Zn-BTC MOFs was prepared by a solvothermal method using zinc as metal and BTC as a

linker. The Zn-BTC was prepared by using different solvents. The solvents that were used were DMF, methanol and DO water. The MOFs prepared from different solvents are then tested for the study of capturing CO₂. After testing it was found that the MOFs prepared from the DMF solvent show the more adsorption capacity as compared to the MOFs prepared from the solvent like ethanol and DI water. This research report also showed us that we can replace the costly solvent with inexpensive solvents without compromising the adsorption capacity.

Barbara S et al. [55] reported the synthesis of Cu (BTC)-MOF. The MOFs were prepared by using solvothermal method. In this method they reported the solvent which was used is DMF. The MOFs were characterized by using different analytical techniques XRD, SEM and FTIR. The Cu (BTC) MOFs shows the high uptake capacity of CO₂ is 9.59 mmol/g.

2.4 HMTA based MOFs

Asgar, Aisha, et al. [56] reported the synthesis of a Cu-BDC metal-organic frameworks (MOFs) was modified through the addition of hexamethylenetetramine (HMTA). These Cu-BDC-HMTA MOFs were created using solvothermal techniques and are designed for CO₂ capture. The resulting material is a crystalline solid characterized by rod-like crystallites. Thermogravimetric analysis indicates that Cu-BDC-HMTA exhibits greater thermal stability compared to Cu-BDC MOFs. Additionally, carbon dioxide adsorption tests demonstrate a significant improvement in CO₂ uptake for the amine-modified framework, with values of 5.25 wt% for Cu-BDC and 21.2 wt% for Cu-BDC-HMTA at 273 K and 1 bar. The introduction of nitrogen atoms through HMTA incorporation contributes to the enhanced CO₂ gas adsorption. Further research is necessary to evaluate the long-term stability of Cu-BDC-HMTA and its resilience to contaminants.

2.5 MOF-5

Wojciech Kukulka et al. [57] reported the synthesis of MOF-5 by using solvothermal method. The MOF-5 was prepared for the adsorption of the CO₂. SEM, XRD, BET, and FTIR techniques were used for studying the physical properties of the MOF. The MOF is undergone for the study of the adsorption capacity of CO₂. The MOF-5 shows excellent adsorption capacity. It shows the 2.43 mmol/g adsorption capacity of the CO₂ at 25 °C and a pressure of 1 bar [43]. A.K. Adhikari et al. [2016] reported the synthesis of two MOFs, the Ni-MOF and the other one is Co-MOF. The MOFs were prepared by using solvothermal methods and are used for the study of the adsorption capacity of CO₂. To enhance the adsorption capacity of the MOFs the Ni and Co MOFs were then doped with palladium (Pd) metal. The MOFs are now after Pd-Ni-MOFs and Pd-Co-MOFs. These MOFs were undergone for the testing of the adsorption of the CO₂, The Pd-Ni-MOF and Pd-Co-MOFs show the adsorption capacity of 12.24 and 11.42 mmol/g respectively.

Yongwei Chen et al. [58] reported the synthesis of Ni based MOFs. Having uniform and ultra-microporous structure. The MOFs were used for the adsorption capacity of the CO₂. The adsorption capacity of the MOFs is 3.11 mmol/g. It is highly selected towards CO₂ and hit is used to remove CO₂ from the natural gas.

Hao Sun et al. [59] reported the synthesis of the nickel based MOFs, they reported the synthesis of Nickel based MOFs using BDC as linker and DMF as a solvent, the MOFs were prepared by using solvothermal method, the MOFs were then used for the study of the water splitting reaction , the results shows the extraordinary results against the water splitting reactions.

2.6 MOF-199

Rana Th. A. Alrubaye et al. [60] reported the synthesis of MOF-199. The MOF-199 was prepared by solvothermal method, including copper cu as a metal and BTC as linker.

This report shows the effects of parameters (solvent, temperature, time) on the adsorption study. The MOFs show high crystalline structure and high surface area. The report shows the adsorption capacity of MOF-199 at different temperatures at a pressure of 1 bar. The results of the report show that the maximum adsorption CO₂ capacity for the MOF-199 is 4 mmol/g at 25 °C.

2.7 MOF-74

Changwei chen et al. [61] reported the synthesis of the Ni based MOFs. The MOFs was named MOF-74. The MOFs were synthesized by both microwave and solvothermal methods. These prepared MOFs from different synthesis methods were then used for the CO₂ adsorption study. The MOFs were also characterized by using techniques like SEM, XRD, FTIR, BET. The research shows that the MOFs preparation is rapid when it is synthesized by using microwave method. The MOFs prepared by microwave method also show high CO₂ adsorption capacity. The MOFs prepared by microwave show 5.52 mmol/g of CO₂ adsorption, while MOFs prepared from solvothermal method show the 3.37 mmol/g of CO₂ adsorption capacity.

2.8 UiO-66

Kasra Pirzadeh et al. [62] reported the synthesis of two MOF, one is UiO-66 and the other one is Cu (BTC)-MOFs, the MOFs UiO-66 was prepared by the solvothermal method, while the MOFs Cu (BTC) was prepared by using electrochemical method. The MOFs were prepared for the testing of the CO₂ adsorption capacity. The MOFs are also characterized by using analytical techniques XRD, SEM, FTIR. The adsorption capacity of the UiO-66 MOF prepared from solvothermal method is 3.32 mmol/g while the adsorption capacity of the Cu (BTC) MOF prepared from electrochemical method is 3.87 mmol/g. The adsorption study of both MOFs occurred at a temperature of the 25 °C and a pressure of 1 bar.

2.9 MOF-200

Maria G. Frysali et al. [63] reported the synthesis of MOF using different functionalized group. They synthesis the MOFs named MOF-200, MOF-210. Among all of the MOFs, the MOF-210 has been reported as the only MOF which has the largest BET surface area, 10400m²/g. The high porosity is achieved when the number of linkers has been also increased. The linkers that are used in MOF-200 are terephthalic acid to (benzene-1,3,5-triyl-tris (benzene-4,1-diyl)) tri-benzoate. The MOF-200 and MOF-210 showed the highest CO₂ adsorption capacity of 54.5 mole/kg at a pressure of 50 bars. At higher pressures the CO₂ adsorption capacity depends on surface area and the pore size of Metal Organic framework (MOF). Increasing the surface area and the pore size and pore volume of the MOF will result in an increase in the adsorption capacity of the MOFs. Organic linkers featuring multiple benzene rings in bulk form have been utilized to create metal-organic frameworks (MOFs) characterized by exceptionally high surface areas and large pore sizes. The performance of these MOFs at ambient temperatures and low pressures is primarily influenced by the properties of their pore surfaces, which exhibit significant functionalization and facilitate substantial material uptake.

2.10 MOF-500

Yongwei Chen et al. [64] reported the synthesis of MOF-505. The MOF-505 was synthesized by using solvothermal method. In order to enhance the adsorption capacity of MOFs. The graphite oxide composite of MOF-505 was prepared. The composites were characterized by using XRD, SEM, FTIR and BET. MOF-505 and its composites were used for the adsorption study of CO₂. It was found that the adsorption of composites is 37.3% greater than the parent MOF-505. Junaid khan et al. [65] reported the synthesis of MOF. The MOF that was used in this report was prepared by using the solvothermal method. The MOF is an amino-functionalized Cu based MOF. The MOF was characterized by using XRD, SEM, FTIR and BET. The MOF undergoes adsorption testing. The MOFs show the CO₂ adsorption capacity of 5.85 mmol/g.

2.11 MOF-74

Qing-Fang Deng et al. [66] reported the synthesis of mesoporous carbon nitride structure for the adsorption of the CO₂. The MOF was prepared by using solvothermal method. It shows high surface area of about 278–338 m²/g, shows the adsorption capacity of 3.05 mmol/g at a pressure of 1 bar. It shows the high selectivity toward CO₂.

Zongbi Bao et al. [67] reported the synthesis of Mg based MOFs. The MOF is named Mg-MOF-74, and it was prepared by using solvothermal method. In MOF-74 the metal was Mg, and the linker used was 2,5-dihydroxyterephthalic acid. The MOFs show a high capturing capacity. The CO₂ adsorption capacity of MOFs is 8.61 mmol/g. This MOF is also used for the adsorption of CH₄ gas with the CO₂ adsorption capacity of 1.05 mmol/g but the results show that this MOF shows the good adsorption capacity toward the CO₂.

Li, Peinan, et al. [53] studied the CO₂ adsorption capability of the amino-modified mesoporous carbon material which was 2.85 mmol/g at 25 °C. This outcome underscores the effective role of dicyandiamide in forming the carbon framework, whereas the next amino modification markedly improves the material's capacity to adsorb CO₂. The produced material possesses a high nitrogen content and displays exceptional selectivity for CO₂. The material has a pore size of 14.5 nm, with a BET specific surface area of 656 m²/g and a pore volume of 0.45 cm³/g.

Ding, Yudong, et al. [29] explored the adsorption of AlFu MOFs enhanced with elevated CO₂ partial pressure and reduced temperature. The CO₂ adsorption capacity of AlFu@CMC-2.5 wt% was 1.26 mmol/g at 35 °C and 1.0 bar pressure. The Avrami kinetic model may more accurately characterize the complex adsorption behavior of AlFu pellets. The CO₂ adsorption rate was ascertained using film diffusion resistance and intraparticle diffusion resistance.

Azhar, Muhammad Haris, et al. [68] studied the Ni-BDC MOF and its composites with g-C₃N₄ which have been effectively synthesized utilizing the solvothermal technique

under CO₂ at 15 bar and 25 °C for adsorption studies of the sample. The Ni-BDC MOF and its composites with g-C₃N₄ exhibit significant adsorption and desorption capabilities. The adsorption capacity of g-C₃N₄ rises to 5 wt% in the g-C₃N₄/Ni-BDC MOF, exhibiting favorable desorption capacity.

2.12 Research Gap

The current research focuses on three dimensional frameworks implied as adsorbents for gas sequestration and storage. However, most of the adsorbing materials either show lower adsorption capacities or volatility which results into the quick desorption owing to the lower thermal stability of the material.

2.13 Problem Statement

Current amine-based solvents exhibit volatility and low absorption capacity, whilst existing adsorbent materials are characterized by low surface area and restricted adsorption capabilities, indicating substantial potential for enhancement.

2.14 Research Objectives

The objectives of the research are on the following points

- To synthesize of Zn BDC MOF and Ni BDC MOF
- To synthesize of Zn BDC HMTA MOF and Ni BDC HMTA MOF
- To characterize of synthesized samples using XRD, SEM, FTIR, TGA, and BET analysis
- To study the CO₂ adsorption capacity of the modified MOF at different pressure and temperature.

CHAPTER 3: INTRODUCTION TO EXPERIMENTAL TECHNIQUES

3.1 Physiochemical Characterization Techniques

The characterizations of the Zn BDC, Ni BDC, Zn BDC HMTA and Ni BDC HMTA have been done by various techniques. The working principle and testing conditions of each technique is discussed below.

- Scanning Electron Microscope (SEM)
- X-Ray Diffraction (XRD)
- X-ray Photoelectron Spectroscopy (XPS)
- Thermo-Gravimetric Analysis (TGA)
- Fourier Transform Infrared Spectroscopy (FTIR)
- Brunauer-Emmett-Teller Analysis (BET)

Scanning electron microscopy was developed in the early 1950's. The main components of Scanning Electron Microscopy are scanning system, detectors, electron column, vacuum system, and display and electronics control. The SEM is an analytical technique that is used to study the structure and the morphology of the MOFs. The resolution of the scanning electron microscope (SEM) that has been used is about 4nm and magnification power of about 10-150,000X. It works on very simple principles. It consists of two Cathode ray tubes. The sample is placed in the first cathode ray tube and the high energy beam of electron is bombarded on the surface of the sample the result of the bombardment is received by the detector and the signals is then converted into the voltages. These voltage signals are now sent to the second cathode ray tube section where it is displayed on the display. The operation of both CRT produces an image which is built up, point to point on CRT display. Secondary, transmitted electrons, backscattered electrons and X-ray detectors produce the signals simultaneously which is employed as

SEM image. The scanning electron microscopy works very fast, it can complete Back Scattered Electron (BSE), SEI and Energy Dispersive X-ray spectroscopy (EDX) analyses, this analysis is done by using a Scanning Electron Microscope (SEM) in less than five minutes. Scanning electron microscopy is user-friendly and easy to operate with the proper training.

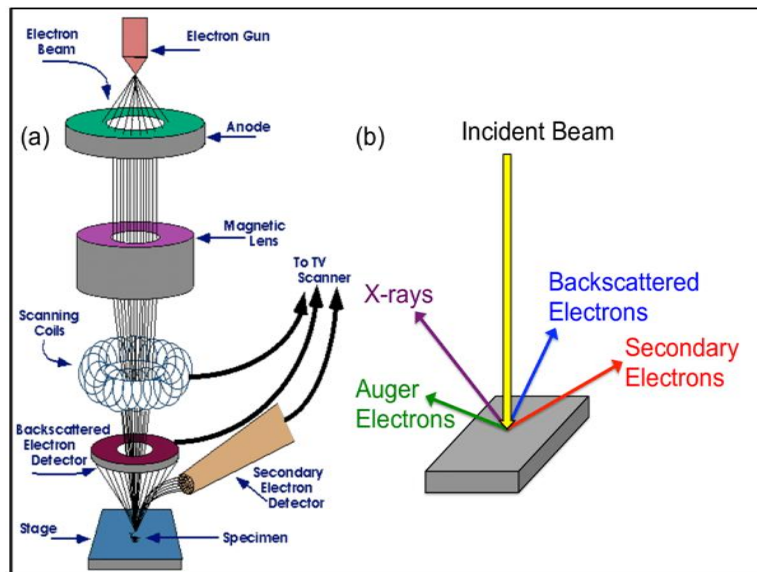


Figure 3.1: Schematic illustration of working of scanning electron microscopy (SEM) [69]

Scanning electron microscopy gives us morphological, topographical, and compositional information. It can also detect and analyze fractures, provide qualitative analyses, and identify crystalline structures. SEM analysis is said to be “nondestructive” as no volume loss has observed during X-rays generation by electrons interaction as electron do not penetrate the sample and they made on surface interaction with the sample, which make it possible to analyze the material repeatedly. Fig 3.1 shows the schematic of the SEM and the main elements of the SEM which includes the electron gun, anode, magnetic lens, scanning coils, secondary electron detectors, TV scanner, magnetic lens.

XRD is a powerful and non-destructive technique. It is an analytical technique which is used to measure the crystallinity of the material. The XRD gives us information about the structure, strain, crystals defects, texture and the structural parameters. It works

on the principle of the brags law $2d \sin\theta = n\lambda$ in the above formula the 'n' denotes the integer values, the ' λ ' denotes the wavelength of the X-rays, 'd' denotes the interplanar spacing generating the diffraction and the ' θ ' denotes the diffraction angle The XRD works on the principle of the constructive interference of the sample which was under examination with monochromatic x-rays. The X-rays were produced from the cathode ray tube, these rays were then passed through the monochromator where the rays were filtered out and only monochromatic waves are heading towards sample.

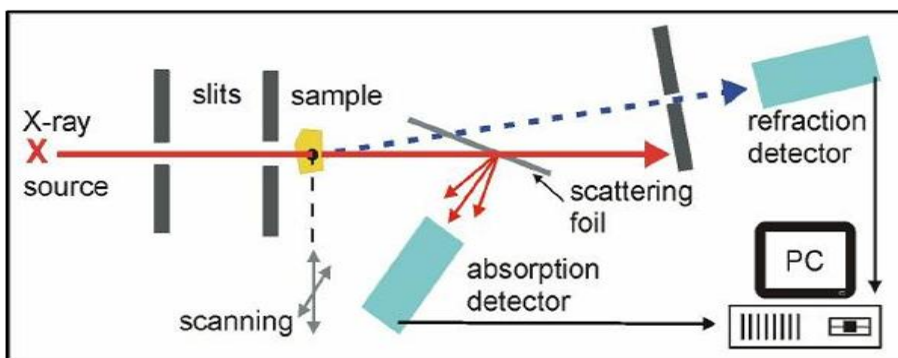


Figure 3.2: Schematic diagram of working of x-ray diffraction spectroscopy [70]

The XRD includes X-ray source through which the X-rays were emitted, slits through which the X-ray and can strike with the sample, after striking with the sample the X ray then reflected from the scattering foil, these scattered rays were then collected and detected by the absorption detector, which is then gives the data, with the help of this data the graphs were drawn.

The Fourier Transform Infrared Spectroscopy (FTIR) is the most widely used analytical technique. It is one of the non-destructive techniques which is used to determine vibrational characteristics of functional groups, and it is also used to identify the type of chemical bonds present and which type of functional groups are present in a molecule by using Infrared radiation. The working of FTIR is simple, the FTIR consists of the light source though which the IR is emitted, beam splitter through which IR beam is slitted and after splitting the beam of IR is passed through the sample which is absorbed by the sample at specific frequencies and then pass through the interferometer and reaches the detector.

The detector converts the signals into voltage and then the signals are amplified and converted to the digital signal. InfraRed spectrum that is obtained as a result is a plot between transmittance (%) and frequency in terms of wavenumbers. In FTIR the sample is placed in a FTIR by making pellets but in modern FTIR there is no need to make sample pellets, the sample can be placed directly into the FTIR. This technique works best as a combination with Fourier transformation.

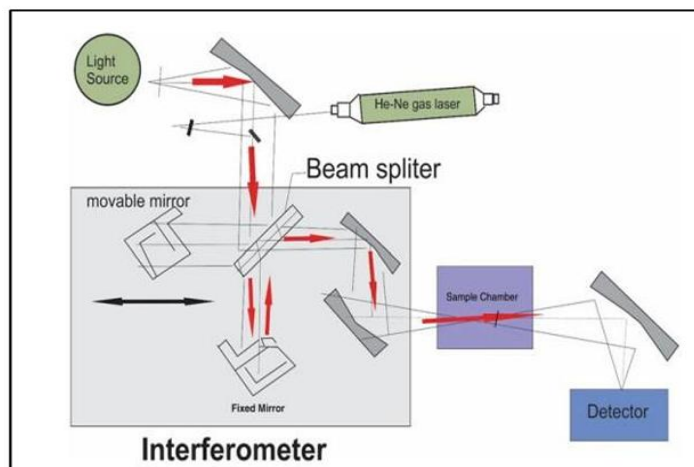


Figure 3.3: Schematic illustration of working of fourier transform infrared (FTIR) spectroscopy [71]

The basic principle of this technique is that the exposure of any compound to low energy infrared rays, results in a change in vibration modes of dipole sites of that compound. As a result, a spectrum is formed showing the corresponding absorption or emission. These results help to evaluate the class to which that compound belongs i.e., carbonyl compound, alcoholic etc. It concurrently collects data over a wide spectral-range and relies on the fact that most of the absorbed light lies in infrared regions of electromagnetic spectrum. Spectrophotometer produces an optical signal with all absorbed or emitted IR frequencies in it in the form of spectrum to evaluate the presence of different groups or classes in the examined compound. So, two types of spectra can be obtained from this technique. The one which is obtained by absorption of IR radiation while the other due to transmitted IR radiation named absorption and transmission spectra respectively. There are two types of the region present in FTIR spectrum, one region is

known as functional group region while the other region is known as the fingerprint region. With the help of the spectrum the functional groups that are present in a sample are detected.

Thermogravimetric analysis is used to predict thermal stability of a sample material. Thermogravimetric analysis can measure amount and the rate of change in weight of sample by increasing temperature in a controlled environment. The temperature is increased at constant rate for a calculated initial weight of the sample and change in sample weight is then recorded as a function of temperature at specified time intervals [Fig. 3.4] [66].

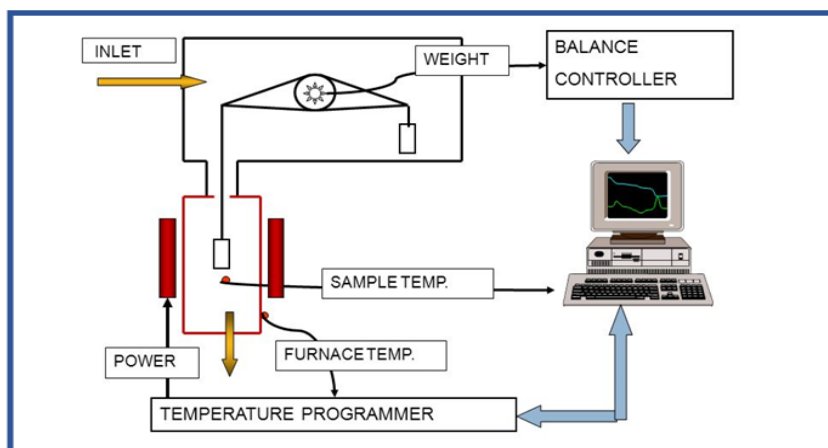


Figure 3.4: Working principle of Thermogravimetric Analysis [72]

BET is named after the first names of its inventors Brunauer-Emmett-Teller. This technique is used for the external surface area evaluation and pore measurements yielding important information about the effects of porosity and particle size properties [4]. The heterogeneous catalysts have individual or more groups of pores whose size and volume are influenced by the method of preparation of catalyst. Fig 3.5 shows the working principle of BET analyzer.

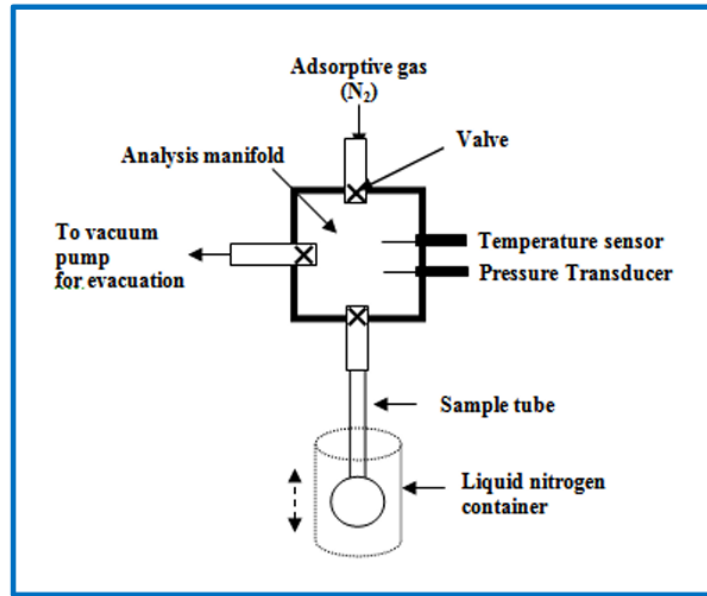


Figure 3.5: Working principle of Brauner-Emmett-Teller (BET) [73]

Nitrogen Adsorption at 77K is the best extensively used technique for surface area analysis and characterization of porous texture. This analysis method uses the nitrogen multilayer physical adsorption studied against change of pressure. The first step is the determination of adsorption isotherm; nitrogen adsorbed volume against its relative pressure. The adsorption isotherm depends upon the porous texture of the solid.

3.2 Physisorption Analysis

The adsorption capacity of the materials is tested and analyzed in order to evaluate the performance of the materials as adsorbents.

Following the characterization and confirmation of material synthesis, comes the application step of the thesis. The prepared MOFs are compared based on how they perform as physical adsorbents for carbon capture. The difference in the solvent effects the crystal structure of each sample and hence the gas adsorption performance. To fulfill this task, high pressure Quanta chrome's iSorbHP1 volumetric sorption analyzer with built-in pumps and sample degassing capability was used (Fig. 3.6) To fulfill this analysis

physical adsorption of a gas on to the surface of solid is determined. The amount of gas adsorbed on to the previously out-gassed sample depends on pressure, temperature, type of gas and size of surface area. The gas and temperature are already selected and then the adsorption isotherms (volume adsorbed as a function of relative pressure) obtained can be used to calculate surface area of the sample [67]. The process starts with degassing the sample to evacuate the pores by the removal of guest molecules. This leads to the better accessibility of open metal sites (OMS) present in the MOF. The degassing temperatures are reached by the help of heating mental. After suitable degassing, the material is cooled down to the desired temperature for analysis. Then the partial pressure of CO₂ (99.999 % pure) increased over the sample gradually. Some quantity of CO₂ is adsorbed by the material and the values of adsorbed volume at certain pressure points are recorded to generate adsorption isothermal. The desorption measured by a step wise reduction in pressure until a low pressure over the sample is achieved.

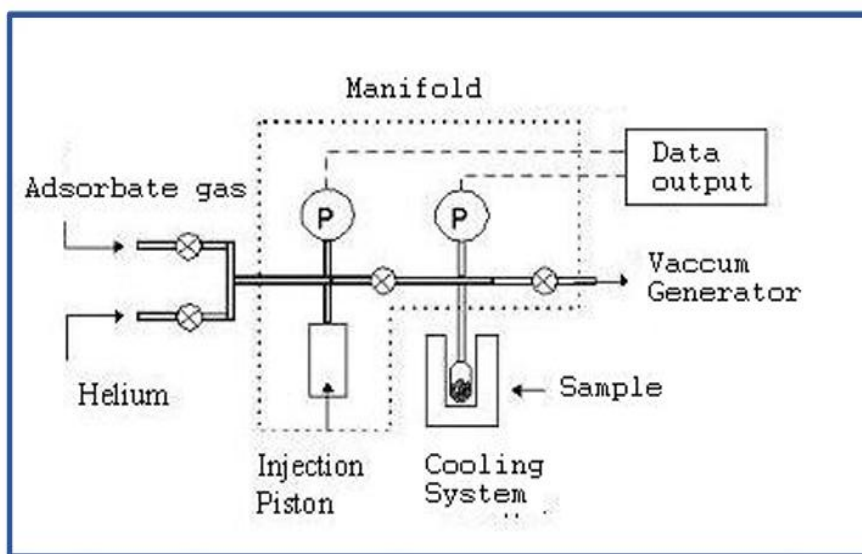


Figure 3.6: Working principle of gas sequestration system [74]

CHAPTER 4: METHODOLOGY

This section elaborates the experimental work carried out in different laboratories and incorporates various suitable synthesis methods used to synthesize desired product. This section describes the synthesis techniques required to produce the desired product. This section explains how Ni-BDC, Zn-BDC, Ni-BDC-HMTA and Zn-BDC-HMTA MOFs were prepared.

4.1 Materials

The chemicals used in the synthesis of MOFs materials were purchased from Sigma Aldrich, UK and Merck, Germany. Chemicals for synthesis include

1. Solvent: Dimethylformamide (DMF) (99%).
2. Organic Linker 1: Terephthalic acid (BDC) 98.9%
3. Organic Linker 2: Hexamethylenetetramine (HMTA)
4. Metal Salts: $\text{Ni}(\text{NO}_3)_2 \cdot 6\text{H}_2\text{O}$, $\text{Zn}(\text{NO}_3)_2 \cdot 6\text{H}_2\text{O}$
5. Washing Solvents: THF (99%) and DMF (99%)

4.2 Equipment

Teflon lined autoclave, Ultrasonication machine, centrifuge machine and vacuum oven.

4.3 Synthesis of MOFs Series

A series of MOFs were prepared by incorporating two metals: Zinc (Zn) and Nickel (Ni).

4.3.1 Zn-BDC⊃HMTA Synthesis

To synthesize Zn-BDC⊃HMTA, equimolar amounts (1:0.5:0.5) of Zn(NO₃)₂·6H₂O (297.49 mg, 1 mmol), terephthalic acid (166 mg, 1 mmol), and hexamethylenetetramine (140 mg, 1 mmol) were dissolved in 10 ml of DMF in a 50 ml beaker. The mixture was subjected to ultrasonication at 25 °C for 30 minutes, after which it was transferred to a 23 ml Teflon vial within a steel Parr vessel. The vessel was sealed and placed in an oven at 110 °C for 24 hours, resulting in the formation of white crystals. Following this, the reaction mixture was decanted, and the product was centrifuged and washed three times with DMF (5 ml each) and then three times with THF (5 ml each), yielding white crystals. Prior to further analysis, the sample was activated in a vacuum oven at 200 °C for 12 hours. The same synthesis approach was employed to obtain Zn-BDC MOF, excluding the HMTA addition [56]. This resulted in white crystals (yield 89 %).

4.3.2 Ni-BDC⊃HMTA Synthesis

To synthesize Ni-BDC⊃HMTA, equimolar amounts (1:1:1) of Ni(NO₃)₂·6H₂O (290.79 mg, 1 mmol), terephthalic acid (166 mg, 1 mmol), and hexamethylenetetramine (140 mg, 1 mmol) were dissolved in 10 ml of DMF within a 50 ml beaker. The mixture underwent ultrasonication at 25 °C for 30 minutes, after which it was transferred to a 23 ml Teflon vial placed inside a steel Parr vessel. The vessel was sealed and subjected to heating in an oven at 110 °C for 24 hours, resulting in the formation of greenish-blue crystals. Afterward, the reaction mixture was decanted, and the product was centrifuged and washed three times with DMF (5 ml each), followed by three washes with THF (5 ml each), producing green crystals. Prior to further analysis, the sample was activated in a vacuum oven at 200 °C for 12 hours. The same synthesis method was applied to produce Ni-BDC MOF without incorporating HMTA [75]. This resulted in green crystals (yields 89%).

CHAPTER 5: RESULTS AND DISCUSSION

5.1 X-Ray Diffraction (XRD)

The x-ray diffraction spectroscopy technique was adopted to analyze the crystal structure of prepared MOFs. The graphs in figures 5.1 and 5.2 show the XRD patterns of Ni/Zn-BDC and HMTA modified Ni/Zn BDC MOFs. The distinctness of the peaks in the diffraction pattern indicates the crystalline nature of the product. Notable metallic peaks are observed at 2θ values of 5.5, 10, 14.2, 15.5, 17, and 21, which correspond to the (hkl) indices of (200), (220), (400), (420), (333), and (600), aligning closely with the simulated pattern of MOF-5 [76]. Additionally, the PXRD pattern of Ni/Zn -BDC \supset HMTA reveals several extra peaks, particularly at $2\theta = 18.7^\circ$, 26.8° , and 31° [77].

This suggests the coordination between the metal and the ligands to form a complex structure. The pattern's clarity, with minimal noise and fewer extraneous peaks, signifies that the resulting products are highly crystalline materials.

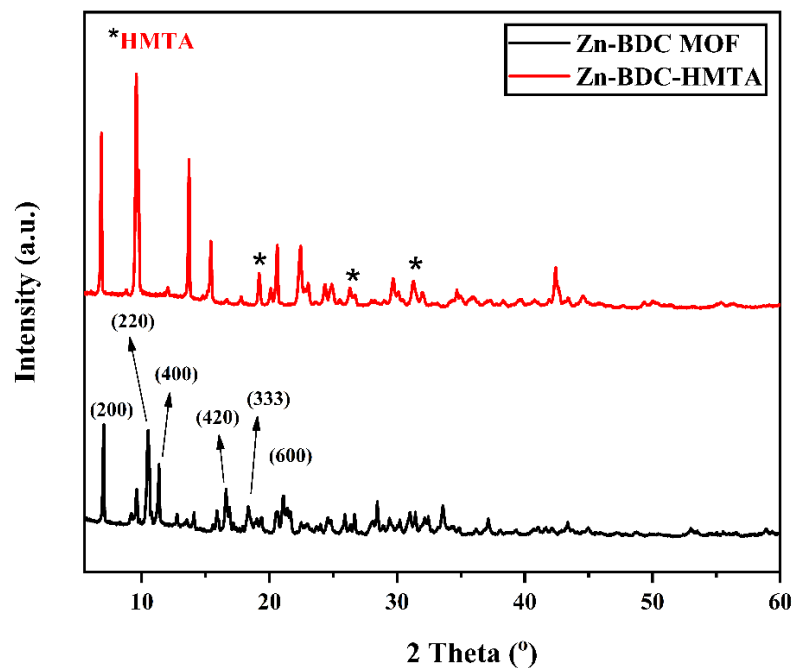


Figure 5.1: XRD pattern of Zn-BDC and HMTA modified Zn-BDC MOFs

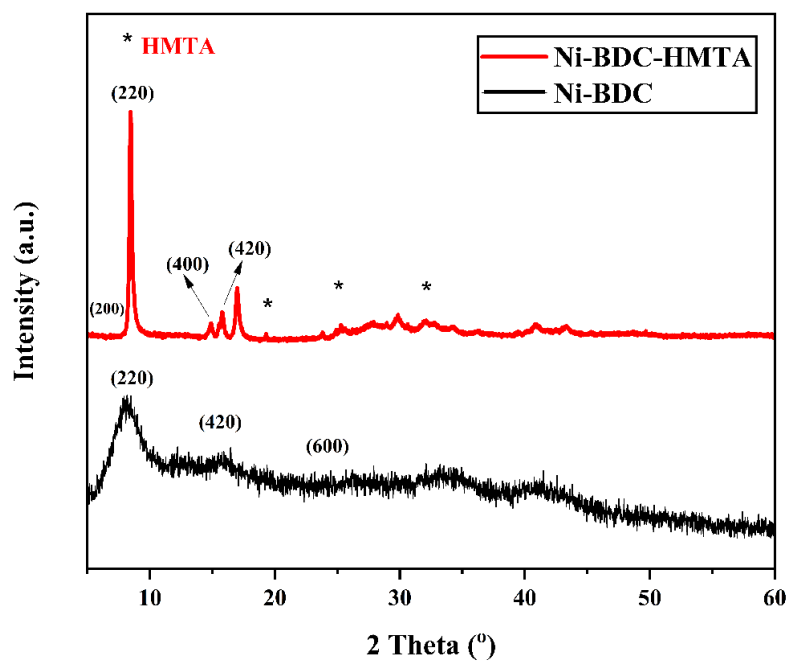


Figure 5.2: XRD pattern of Ni-BDC and HMTA modified Ni-BDC MOFs

5.2 Scanning Electron Microscope (SEM)

The Scanning Electron Microscopy (SEM) is done in order to know the structure and the morphology of samples. Before doing the SEM, the samples first gets dried under vacuum oven, and then after drying the dried samples were coated by gold with the help of sputter coater to avoid the charging of the materials. The SEM analysis was done using 20kV SEM.

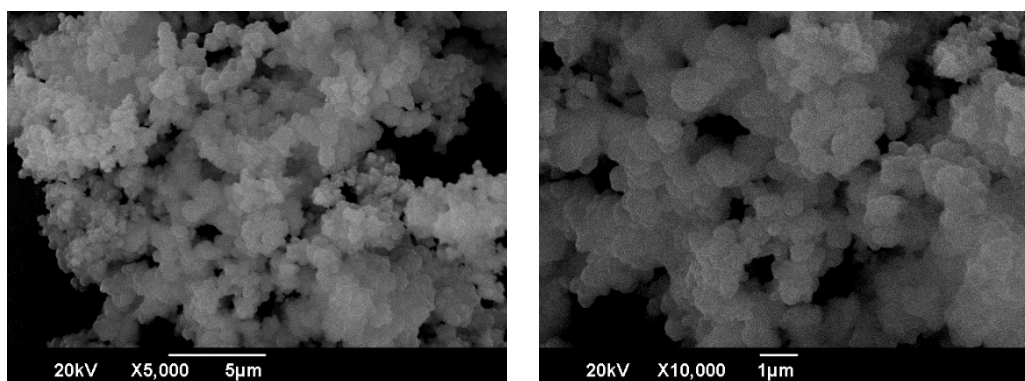


Figure 5.3: SEM images representing the morphology of Ni-BDC

The SEM images of Ni-BDC and Ni-BDC-HMTA MOFs were taken at different magnifications of 1 μm and 5 μm in order to get detailed study of the crystal structure and morphology. The SEM shows the 2D structure of the samples.

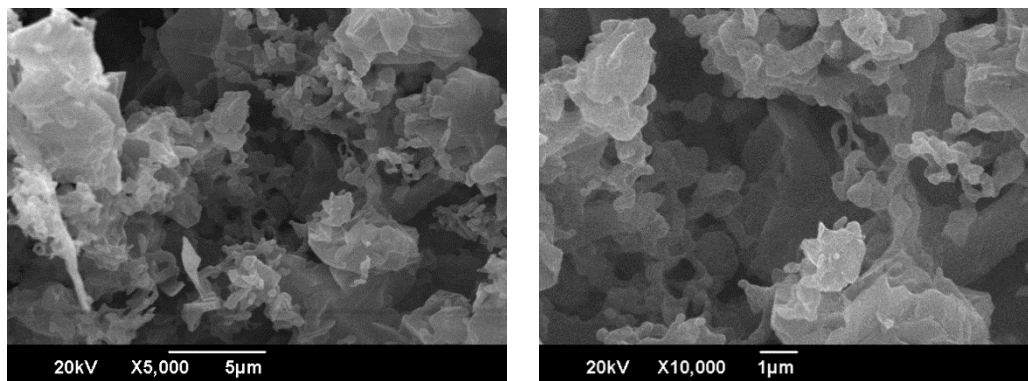


Figure 5.4: SEM images representing the morphology of Ni-BDC-HMTA

From SEM, Ni-BDC appears like irregular microspheres with large voids as shown in figure 5.3 (a-b) whereas, when Ni-BDC modified with HMTA linker surface morphology changes, a catalyst looks like sheets interlinked with each other shown in figure 5.4 (a-b) [78].

5.3 Fourier Transform Infrared Spectroscopy (FTIR)

The FTIR study shows the presence of functional groups, and the types of bonds present in samples. Before doing the FTIR we make pellets of our samples. The pallets were placed in FTIR. The FTIR results are obtained in the form of a spectrogram which is a graph between wave number (cm^{-1}) and transmittance (%).

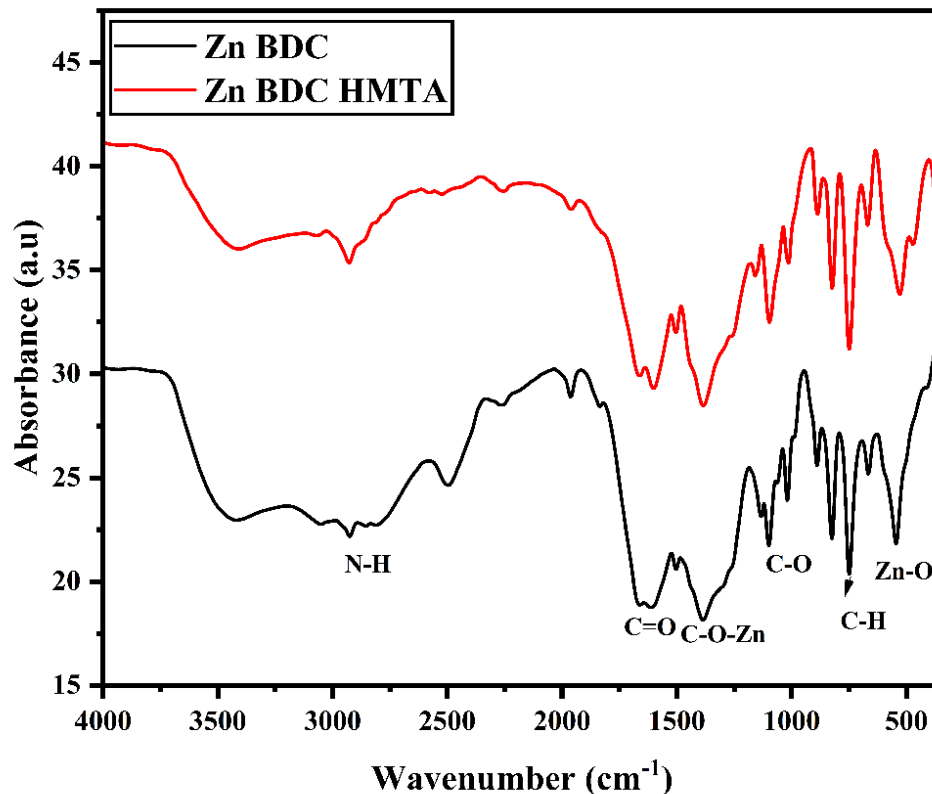


Figure 5.5: FTIR Spectrum of Zn-BDC and HMTA modified Zn-BDC representing all the bands corresponding to different metallic and non-metallic bonds available in the structure

Fourier transform infrared spectroscopy studies were performed on prepared to sample to get an idea about functional groups present in the samples that will be indicative of success of MOFs material synthesis. The Fourier Transform Infrared (FTIR) spectra obtained for the synthesized materials confirm the existence of characteristic functional groups associated with the formation of Zn-BDC MOF (Fig. 5.5). Distinct peaks corresponding to the symmetric and asymmetric stretching of C-O bonds linked to Zn were observed at 1384 cm^{-1} in the Zn-BDC MOF. A small peak at 3400 cm^{-1} in Zn-BDC MOFs represents adsorbed O-H groups. In addition, HMTA in Zn-BDC MOF Characteristic peak for amine-containing functional groups at 2927 cm^{-1} indicates N-H bond stretching.

Typical peaks at 748 cm^{-1} and 823 cm^{-1} are ascribed to stretching vibration of C-H bonds introduced by amine functional group. Moreover the band at 528 cm^{-1} show the presence of Zn-O stretching bond in our samples [79, 80].

Table 5.1: FTIR bands corresponding to different bonds available in the Zn-BDC-HMTA MOF structure

Functional groups	Peaks values	Functional groups	Peaks values
Zn-O	528 cm^{-1}	C-O-Zn	1384 cm^{-1}
C-H	$748, 823\text{ cm}^{-1}$	C=O	1601 cm^{-1}
C-O	1096 cm^{-1}	N-H	2927 cm^{-1}

Fourier transform infrared spectroscopy studies were performed on prepared to get an idea about functional groups present in the samples that will be indicative of success of MOFs material synthesis.

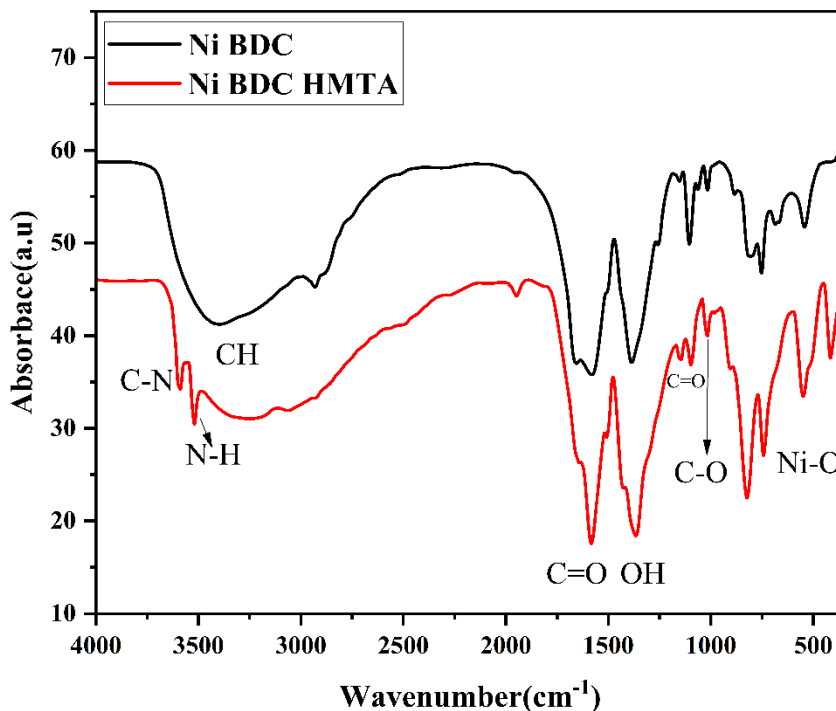


Figure 5.5: FTIR Spectrum of Ni-BDC and HMTA modified Ni-BDC representing all the bands corresponding to different metallic and non-metallic bonds available in the structure

The FTIR analysis of the synthesized materials confirmed the presence of functional groups characteristic of Ni-BDC MOF formation. A band observed at 542 cm^{-1} indicates the existence of Ni-O stretching bonds in the samples. Additionally, distinct peaks representing the symmetric and asymmetric stretching of C-O bonds associated with Ni are noted at 1015 cm^{-1} in the Ni-BDC sample. A sharp peak at 1583 cm^{-1} corresponds to the symmetric and asymmetric stretching of C=O. Furthermore, the inclusion of HMTA in the Ni-BDC MOFs is indicated by a characteristic peak for amine functional groups at 3526 cm^{-1} , which signifies N-H bond stretching [68, 75].

Table 5.2: FTIR bands corresponding to different bonds available in the Ni-BDC-HMTA MOF structure

Functional groups	Peaks values	Functional groups	Peaks values
Ni-O	528 cm ⁻¹	C-O-Ni	1384 cm ⁻¹
C-H	748, 823 cm ⁻¹	C=O	1601cm ⁻¹
C-O	1096 cm ⁻¹	N-H	2927 ⁻¹

5.4 Thermo-Gravimetric Analysis (TGA)

Thermogravimetric analysis (TGA) was conducted to investigate the thermal properties of the synthesized MOF materials (Fig. 5.7). Both MOFs exhibited a weight loss of 19% below 180 °C, suggesting the presence of surface-adsorbed moisture, DMF, and other solvent molecules. The initial weight reduction observed in both samples between 180 °C and 318 °C (approximately 20%) is attributed to the degradation of surface-adsorbed DMF molecules [80]. In the case of Zn-BDC MOFs, the decomposition of the carboxylic linker commenced at 420 °C, whereas for Zn-BDC⊃HMTA MOFs, linker degradation began at a slightly higher temperature of 461 °C, followed by a rapid decline in weight for both materials. Above 487 °C for Zn-BDC MOFs and 520 °C for Zn-BDC⊃HMTA MOFs, no additional weight loss was recorded, indicating the formation of residual zinc oxide [56, 79].

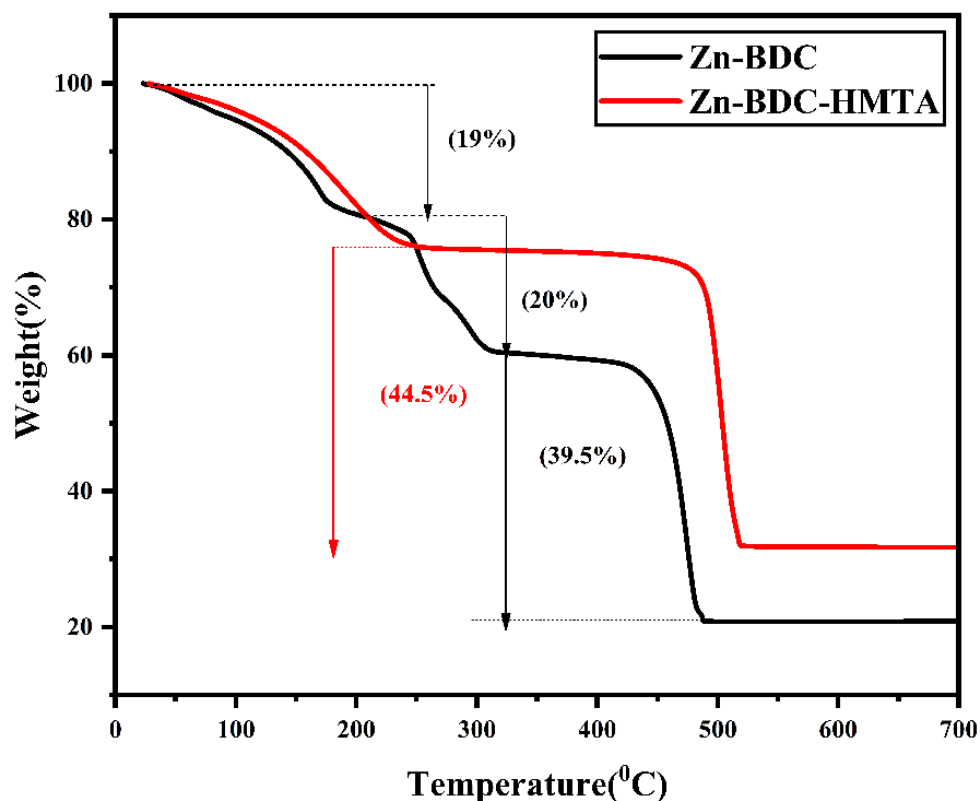


Figure 5.7: TGA profile of Zn-BDC and HMTA modified Zn-BDC representing mass loss trend with increasing temperature

Thermal behaviors of prepared crystals were studied using Thermogravimetric analysis (Fig. 5.8). The samples were subjected to heating from ambient temperature to 700 °C at a rate of 10 °C per minute while maintaining a nitrogen atmosphere. A weight loss of 6.5% was noted for both MOFs below 110 °C, suggesting the presence of surface-adsorbed moisture, THF, and other solvent molecules in the synthesized materials. The initial weight reduction observed in both samples between 110 °C and 312 °C (approximately 36%) is indicative of the degradation of surface-adsorbed DMF molecules [87]. residual nickel oxide above 366 °C for Ni-BDC MOFs and 406 °C for Ni-BDC-HMTA MOFs [81].

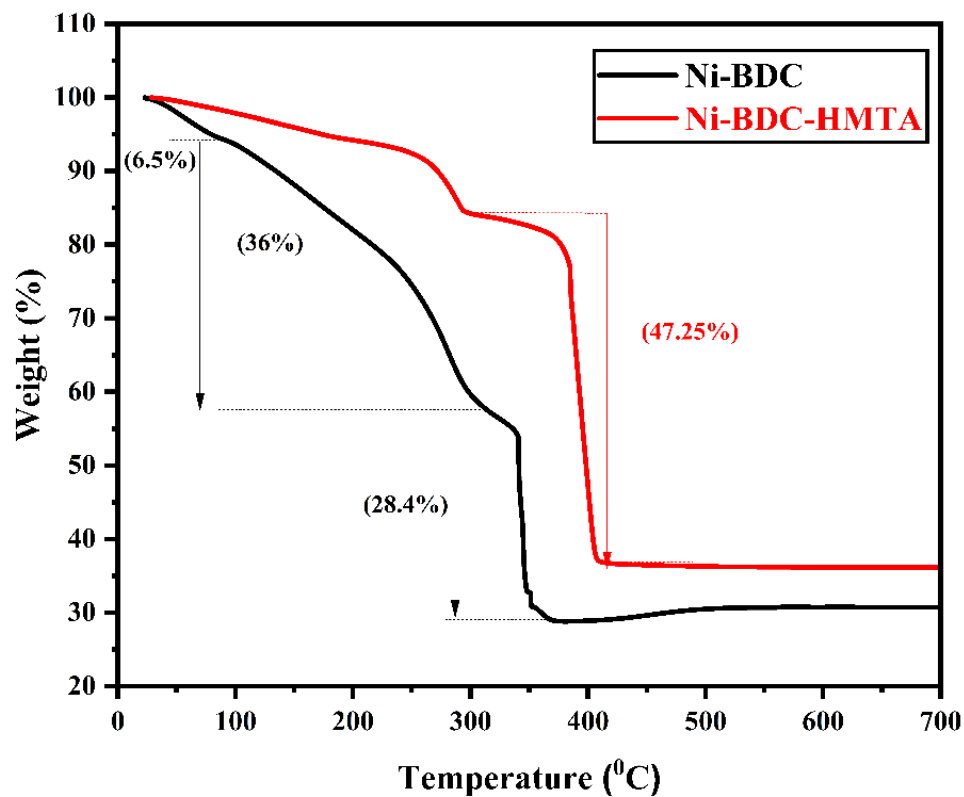


Figure 5.8: TGA profile of Ni-BDC and HMTA modified Ni-BDC representing mass loss trend with increasing temperature

In the case of Ni-BDC MOFs, the decomposition of the carboxylic linker began at 330 °C. In contrast, for Ni-BDC-HMTA, the degradation of the linker commenced at a slightly elevated temperature of 364 °C. Following these points, both materials exhibited rapid degradation. No additional weight loss was detected as the temperature increased further.

5.5 Brunauer-Emmett-Teller Analysis (BET)

The surface area and pore size Zn BDC \supset HMTA MOFs is 66.53 m²g⁻¹ (Fig. 5.9) and 3.54 nm (Fig. 5.10).

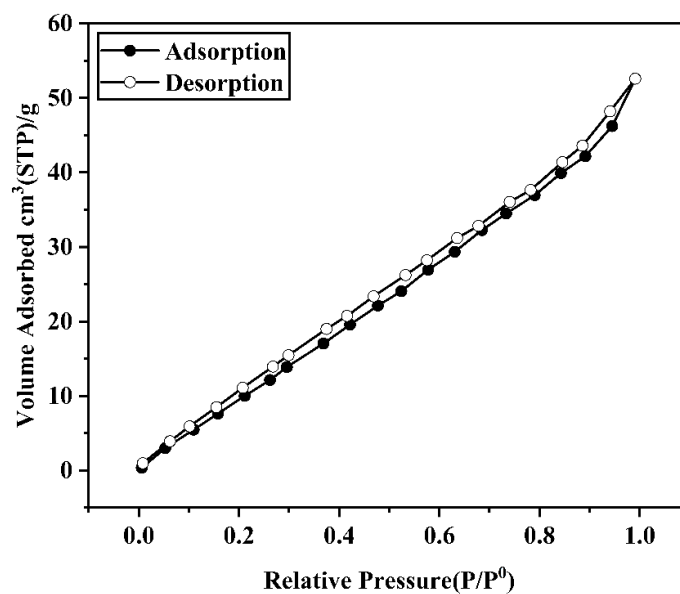


Figure 5.9: N₂ adsorption and desorption isotherms for Zn BDC \supset HMTA MOFs

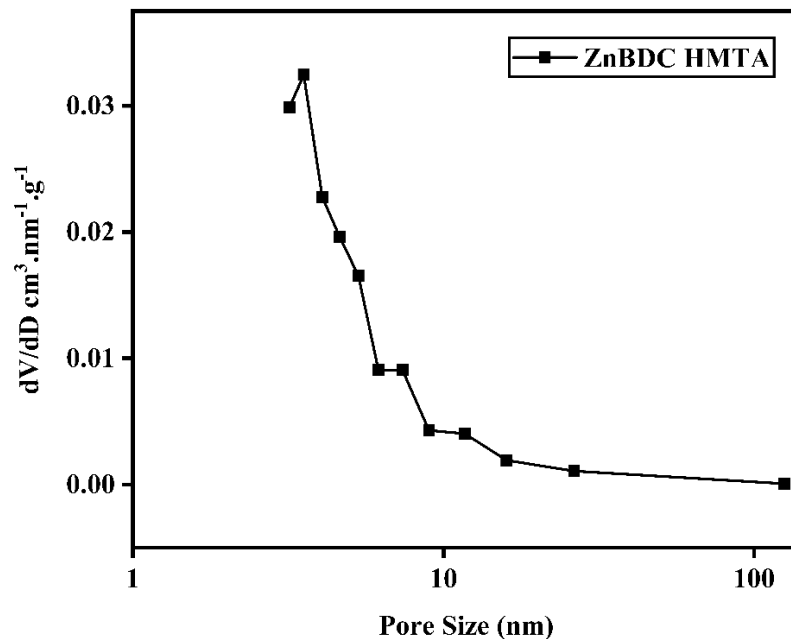


Figure 5.10: Pore size distribution of Zn-BDC-HMTA MOFs

The BET was done for both the Ni BDC and Ni BDC-HMTA MOFs. The pore volume curves are shown in figure 5.12. The surface area and pore size of Ni BDC and Ni BDC-HMTA MOFs is $21.763 \text{ m}^2\text{g}^{-1}$, 3.23 nm (Fig. 5.11 and 5.12) and $220.910 \text{ m}^2\text{g}^{-1}$, 3.16 nm (Fig. 5.13 and 5.14), respectively [82, 83].

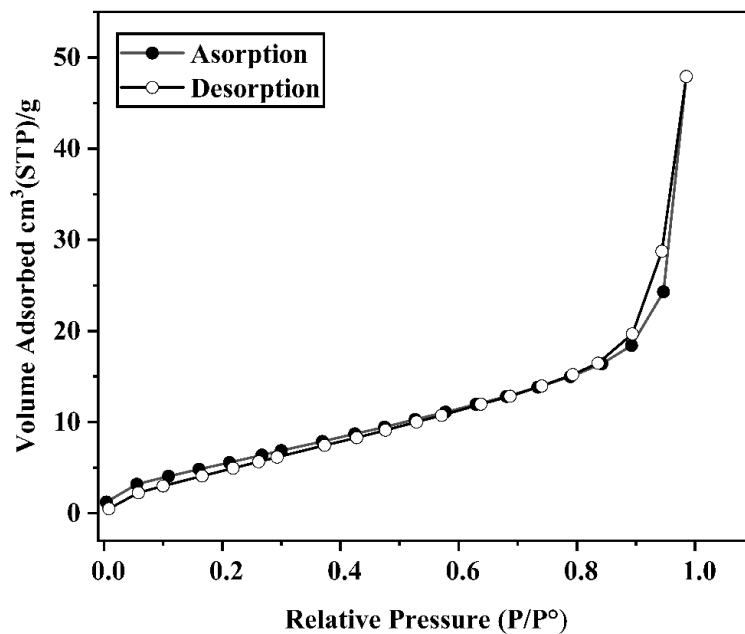


Figure 5.11: N₂ adsorption and desorption isotherms for Ni-BDC MOFs

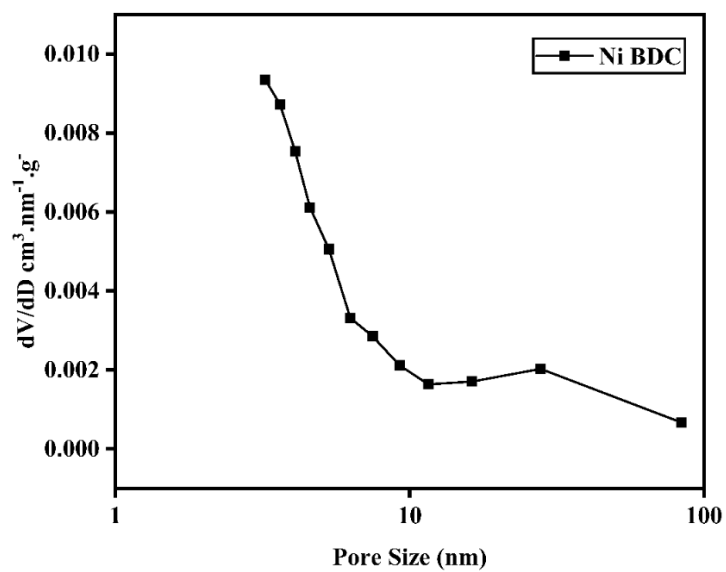


Figure 5.12: Pore size distribution of Ni-BDC MOFs

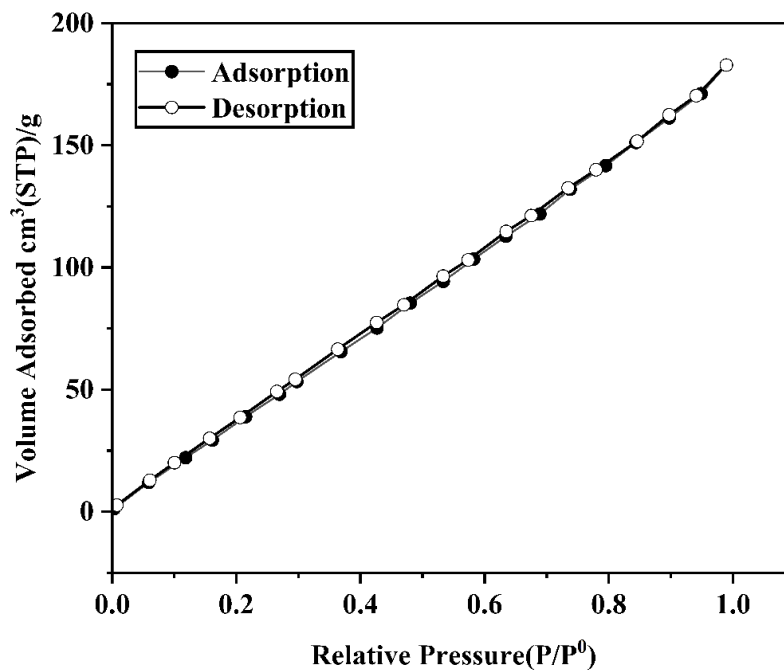


Figure 5.13: N₂ adsorption and desorption isotherm of Ni-BDC-HMTA MOFs

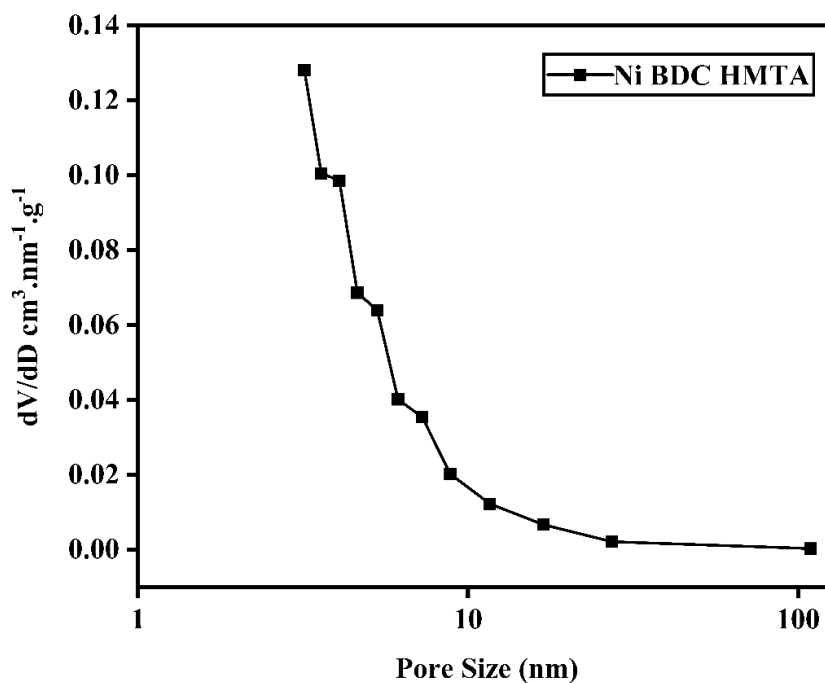


Figure 5.14: Pore size distribution of Ni-BDC-HMTA MOFs

5.6 X-ray Photoelectron Spectroscopy (XPS)

The XPS survey spectra in Fig. 5.15 offers substantial insights into the quality and content of the crystals modified with HMTA.

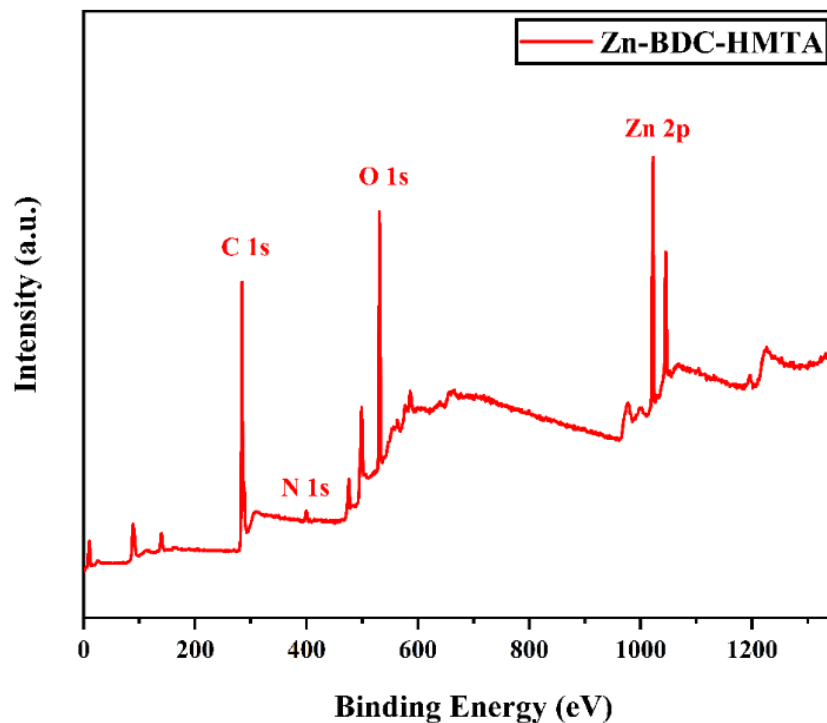


Figure 5.15: XPS survey scan of Zn-BDC-HMTA MOF representing all the necessary identifying peaks

XPS peaks indicate the binding state of the composition of Zn, O as well as C and N corresponding to their bonding in HMTA-modified Zn-BDC MOF. In Fig. 5.16 (a), two prominent peaks are observed at 1021.1 eV and 1044.2 eV, corresponding to the binding energies of Zn $2p_{3/2}$ and Zn $2p_{1/2}$, respectively. The results reveal that the chemical valence of Zn is in the +2 oxidation state [84].

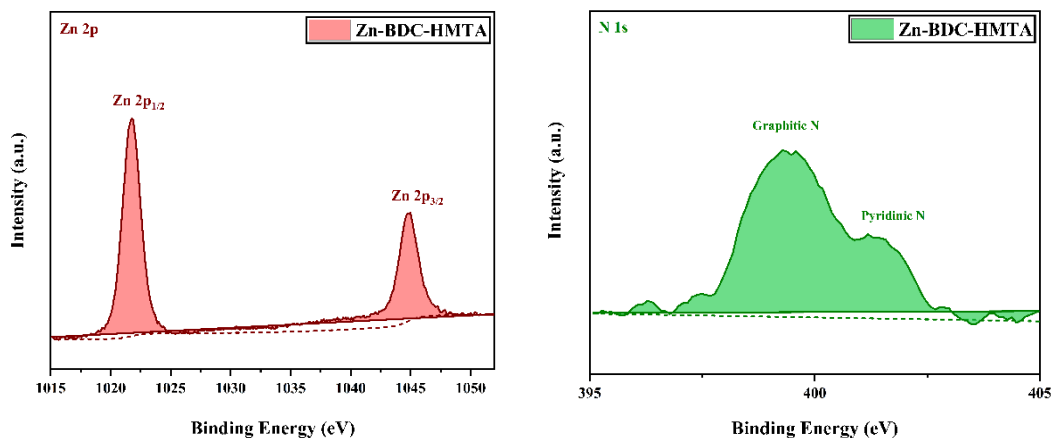


Figure 5.16: XPS B.E plot of (a) Zn 2p and (b) N 1s in Zn-BDC-HMTA MOF

Figure 5.16 (b) illustrates the N1s spectra describing the chemical valence state of Nitrogen in HMTA. The N1s spectra of HMTA can be deconvoluted into two major peaks corresponding to pyridinic N (402 eV), and graphitic N (399.6 eV) [84-86].

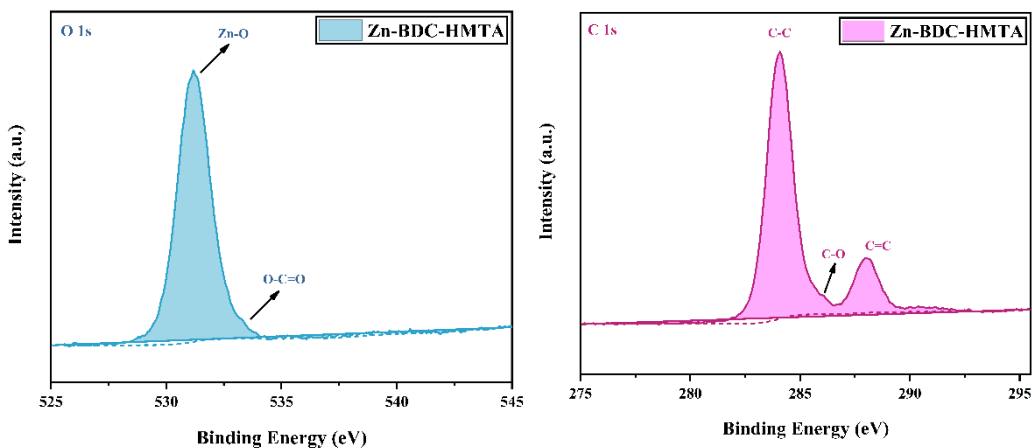


Figure 5.17: XPS B.E plot of (a) O 1s and (b) C 1s in Zn-BDC-HMTA MOF

The deconvolution of the XPS spectra for the O1s core level line is illustrated in Fig. 5.17 (a) corresponding to the presence of oxygen bonding majorly with zinc and

carbon [84]. The B.E plot for C1s represented in Fig. 5.17 (b) corresponds to C-C, C=C and C-O bonding [84, 85].

5.7 CO₂ Adsorption Study of MOFs

High Pressure Gas Sorption Analyzer (iSorp HP1) was used to test the adsorption capacity of the MOFs. For this purpose, the CO₂ adsorption was measured at varying temperatures and pressures. Both the Ni and Zn based MOFs with HMTA and without HMTA were tested, specifically to study the effect of addition of the linker in the MOFs. All analysis were performed at two different temperature 283 K and 293 K between pressures range of 1-14 bar to achieve the adsorption isotherms [87]. The Zn-BDC, Zn-BDC-HMTA, Ni-BDC and Ni-BDC-HMTA MOFs showed (Fig. 4.16) a CO₂ adsorption capacity at 283 K are 1.95 mmol/g, 3.50 mmol/g, 2.15 mmol/g and 2.85 mmol/g respectively. Similarly, the CO₂ adsorption capacity at 293 K are 1.00 mmol/g, 2.15 mmol/g, 2.00 mmol/g and 2.20 mmol/g respectively.

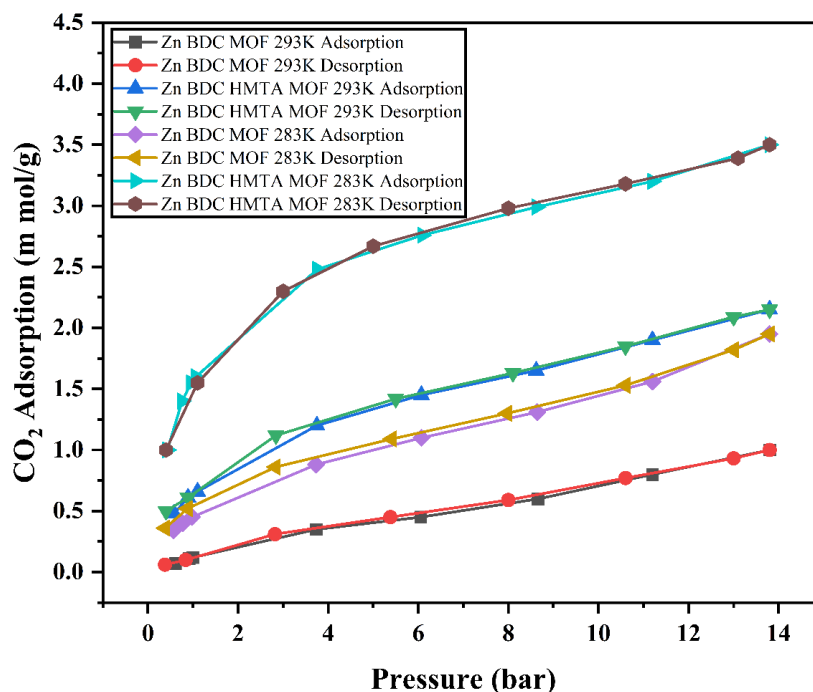


Figure 5.18: CO₂ isotherms of Zn-BDC and Zn-BDC-HMTA at 283 K and 293 K

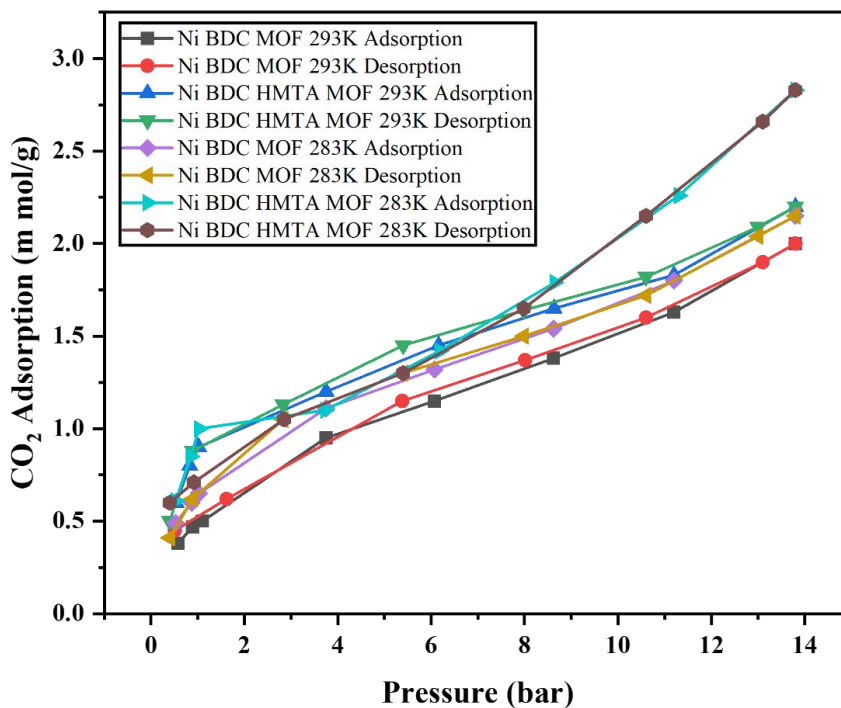


Figure 5.19: CO₂ isotherms of Ni-BDC and Ni-BDC⇒HMTA at 283 K and 293 K

The results of HMTA modified MOFs are significantly greater than without HMTA modified MOFs [56]. The tabular comparison shows that the HMTA modified Zn-BDC and Ni-BDC MOFs have showed better performance with higher values of CO₂ adsorption capacity in comparison to the BDC based single-linker MOFs [88].

Table 5.3: CO₂ adsorption capacity of all the zinc and nickel-based MOFs with BDC and HMTA modified MOFs at different temperature conditions

Sr No.	MOFs	Adsorption (mmol/g)	Temperature (K)	Pressure (bar)
1	Zn-BDC	1.95	283	14
2	Zn-BDC	1.00	293	14
3	Zn-BDC-HMTA	3.50	283	14
4	Zn-BDC-HMTA	2.15	293	14
5	Ni-BDC	2.15	283	14
6	Ni-BDC	2.00	293	14
7	Ni-BDC-HMTA	2.85	283	14
8	Ni-BDC-HMTA	2.20	293	14

The Comparison of the data from this study with the recent reports is also shown in the table 5.4.

Table 5.4: CO₂ adsorption capacity and BET surface area of different MOFs reported in comparison with the synthesized MOFs for this study

Sr No.	MOFs	Adsorption (mmol/g)	BET surface area (m ² /g)	Ref
1	Co BDC	0.67	17.9	[52]
2	Zn BDC	0.95	37.8	[52]
3	Ni BDC	0.069	---	[89]
4	5 wt% g-C ₃ N ₄ /Ni-BDC	0.50	---	[90]
5	Cu-BDC	1.2	---	[77]
6	Cu-BDC⊃HMTA	12	935	[77]
7	Zn BDC	1.95	---	This work
8	Zn BDC HMTA	3.50	66.53	This work
9	Ni BDC	2.15	21.76	This work
10	Ni BDC HMTA	2.85	220.91	This work

The MOFs show a great surface area which is because of the addition of the amine-based linker (HMTA). The enhanced surface area is the reason why the MOFs show good

adsorption capacities as well. The surface area without amine modification of Zn-BDC and Ni-BDC MOFs is 37.8 m²/g and 21.76 m²/g but with amine modification is 66.53 m²/g and 220.91 m²/g. The Zn-BDC and Ni-BDC modified with HMTA provide high adsorption for CO₂. The findings indicate that Zn-BDC-HMTA MOF shows a CO₂ adsorption capability of 3.50 mmol/g, whereas the Ni-BDC-HMTA MOF have a CO₂ adsorption capability of 2.8 mmol/g. Both these capacities are good and are much better as compared to the unmodified MOFs like Zn-BDC and Ni-BDC MOFs which show an adsorption capability of 0.95 mmol/g [52] and 0.069 mmol/g [89].

CHAPTER 6: CONCLUSION AND FUTURE RECOMMENDATION

This detailed research of the selected MOFs produced some really good results and several valuable findings in terms of both synthesis and application.

6.1 Conclusion

1. The Zn BDC and Ni BDC modified with HMTA MOFs provide high adsorption for CO₂. The results show that the Zn BDC HMTA MOFs shows a CO₂ adsorption capacity of 3.50 mmol/g while the Ni BDC HMTA MOFs shows a CO₂ adsorption capacity of 2.8 mmol/g.
2. Both these capacities are good and are much better compared to some of the other without modified MOFs like Zn BDC and Ni BDC MOFs which show an adsorption capacity of 0.95 mmol/g and 0.069 mmol/g, respectively [52].
3. The MOFs show a high surface area which is because of the addition of the amine-based linker (HMTA). The enhanced surface area is the reason why the MOFs show good adsorption capacities as well. The surface area without amine modification of Zn BDC and Ni BDC MOFs is 37.8 m²/g and 21.76 m²/g but with amine modification is 66.53 m²/g and 220.91 m²/g [91].

6.2 Recommendations

The current study focused on the synthesis and effect of Amine Based Metal Organic Frameworks. These experiments can be:

1. The use of different solvents for the synthesis of the MOFs and a comparative study of their adsorption capacities.

2. Studying the effect of change of metal in Amine based MOFs by using 4 to 5 or more different metals for the synthesis and comparing the adsorption and surface area results

Furthermore, a financial study could be conducted to analyze similar MOFs available in literature and to compare the price to performance ratio of all these MOFs.

REFERENCES

1. Criqui, P. and N. Kouvaritakis, World energy projections to 2030. *International journal of global energy issues*, 2000. **14**(1-4): p. 116-136.
2. Olivier, J.G., K. Schure, and J. Peters, Trends in global CO₂ and total greenhouse gas emissions. PBL Netherlands Environmental Assessment Agency, 2017. **5**: p. 1-11.
3. Moazzem, S., M. Rasul, and M. Khan, A review on technologies for reducing CO₂ emission from coal fired power plants. Vol. 11. 2012: chapter.
4. El Zein, A.L. and N.A. Chehayeb, The effect of greenhouse gases on earth's temperature. *International Journal of Environmental Monitoring and Analysis*, 2015. **3**(2): p. 74.
5. Johnson, R.L., *The Greenhouse Effect: Life on a Warmer Planet*. 1993: Lerner Publications.
6. Garfin, G., et al., Assessment of climate change in the southwest United States: a report prepared for the National Climate Assessment. 2013.
7. Ollila, A., Natural Climate Drivers Dominate in the Current Warming. *Science of Climate Change*, 2023. **3**(3): p. 290-326.
8. Kweku, D.W., et al., Greenhouse effect: greenhouse gases and their impact on global warming. *Journal of Scientific research and reports*, 2018. **17**(6): p. 1-9.
9. Lee, S.-Y. and S.-J. Park, A review on solid adsorbents for carbon dioxide capture. *Journal of Industrial and Engineering Chemistry*, 2015. **23**: p. 1-11.
10. Krieger, G., et al., Numerical simulation of oxy-fuel combustion for gas turbine applications. *Applied Thermal Engineering*, 2015. **78**: p. 471-481.
11. Alper, E. and O.Y. Orhan, CO₂ utilization: Developments in conversion processes. *Petroleum*, 2017. **3**(1): p. 109-126.
12. Rubin, E.S., et al., The outlook for improved carbon capture technology. *Progress in Energy and Combustion Science*, 2012. **38**(5): p. 630-671.
13. Songolzadeh, M., et al., Carbon dioxide separation from flue gases: a technological review emphasizing reduction in greenhouse gas emissions. *The Scientific World Journal*, 2014. **2014**(1): p. 828131.

14. Victor, E. and U. Great C, The Role of Alkaline/alkaline Earth Metal Oxides in CO₂ Capture: A Concise Review. *Journal of Energy Research and Reviews*, 2021. **9**(3): p. 46-64.
15. Chen, H., C. Zhao, and Y. Yang, Enhancement of attrition resistance and cyclic CO₂ capture of calcium-based sorbent pellets. *Fuel processing technology*, 2013. **116**: p. 116-122.
16. Li, L., et al., A review of research progress on CO₂ capture, storage, and utilization in Chinese Academy of Sciences. *Fuel*, 2013. **108**: p. 112-130.
17. Ghoniem, A.F., Z. Zhao, and G. Dimitrakopoulos, Gas oxy combustion and conversion technologies for low carbon energy: Fundamentals, modeling and reactors. *Proceedings of the Combustion Institute*, 2019. **37**(1): p. 33-56.
18. Ma'mum, S., et al., Selection of new absorbents for carbon dioxide capture, in *Greenhouse Gas Control Technologies 7*. 2005, Elsevier. p. 45-53.
19. Chai, S.Y.W., L.H. Ngu, and B.S. How, Review of carbon capture absorbents for CO₂ utilization. *Greenhouse Gases: Science and Technology*, 2022. **12**(3): p. 394-427.
20. Ghazvini, M.F., et al., Investigation of the MOF adsorbents and the gas adsorptive separation mechanisms. *Journal of Environmental Chemical Engineering*, 2021. **9**(1): p. 104790.
21. Lai, J.Y., L.H. Ngu, and S.S. Hashim, A review of CO₂ adsorbents performance for different carbon capture technology processes conditions. *Greenhouse Gases: Science and Technology*, 2021. **11**(5): p. 1076-1117.
22. Khamis, F., et al., Comprehensive review on pH and temperature-responsive polymeric adsorbents: Mechanisms, equilibrium, kinetics, and thermodynamics of adsorption processes for heavy metals and organic dyes. *Chemosphere*, 2023: p. 140801.
23. Ochedi, F.O., et al., Carbon dioxide capture using liquid absorption methods: a review. *Environmental Chemistry Letters*, 2021. **19**(1): p. 77-109.
24. Lyu, H., et al., Carbon dioxide capture chemistry of amino acid functionalized metal-organic frameworks in humid flue gas. *Journal of the American Chemical Society*, 2022. **144**(5): p. 2387-2396.
25. Liang, J., et al., Dislocated bilayer MOF enables high-selectivity photocatalytic reduction of CO₂ to CO. *Advanced materials*, 2023. **35**(10): p. 2209814.

26. Ghanbari, T., F. Abnisa, and W.M.A.W. Daud, A review on production of metal organic frameworks (MOF) for CO₂ adsorption. *Science of The Total Environment*, 2020. **707**: p. 135090.
27. Issar, U. and R. Arora, Theoretical Study on Catalytic Capture and Fixation of Carbon Dioxide by Metal–Organic Frameworks (MOFs), in *Metal-Organic Frameworks (MOFs) as Catalysts*, S. Gulati, Editor. 2022, Springer Nature Singapore: Singapore. p. 237-264.
28. Shabir, F., et al., Recent updates on the adsorption capacities of adsorbent-adsorbate pairs for heat transformation applications. *Renewable and Sustainable Energy Reviews*, 2020. **119**: p. 109630.
29. Ding, Y., et al., Synthesis and CO₂ adsorption kinetics of Aluminum Fumarate MOFs pellet with high recovery. *Energy*, 2023. **263**: p. 125723.
30. He, T., X.-J. Kong, and J.-R. Li, Chemically stable metal–organic frameworks: rational construction and application expansion. *Accounts of Chemical Research*, 2021. **54**(15): p. 3083-3094.
31. Mehek, R., et al., Metal–organic framework based electrode materials for lithium-ion batteries: a review. *RSC advances*, 2021. **11**(47): p. 29247-29266.
32. Paul, A., A. Karmakar, and A.J. Pombeiro, Aspects of Hydrothermal and Solvothermal Methods in MOF Chemistry, in *Synthesis and Applications in Chemistry and Materials: Volume 11: Metal Coordination and Nanomaterials*. 2024, World Scientific. p. 281-312.
33. Klinowski, J., et al., Microwave-assisted synthesis of metal–organic frameworks. *Dalton Transactions*, 2011. **40**(2): p. 321-330.
34. Varsha, M. and G. Nageswaran, Direct electrochemical synthesis of metal organic frameworks. *Journal of The Electrochemical Society*, 2020. **167**(15): p. 155527.
35. Główniak, S., et al., Recent developments in sonochemical synthesis of nanoporous materials. *Molecules*, 2023. **28**(6): p. 2639.
36. Troyano, J., et al., Spray-drying synthesis of MOFs, COFs, and related composites. *Accounts of chemical research*, 2020. **53**(6): p. 1206-1217.
37. Raja, D.S. and D.-H. Tsai, Recent Advances in Continuous Flow Synthesis of Metal-Organic Frameworks and Their Composites. *Chemical Communications*, 2024.

38. Sud, D. and G. Kaur, A comprehensive review on synthetic approaches for metal-organic frameworks: From traditional solvothermal to greener protocols. *Polyhedron*, 2021. **193**: p. 114897.
39. Dzhardimalieva, G.I. and I. E. Uflyand, Coordination Polymers Containing Metal Chelate Units, in *Chemistry of Polymeric Metal Chelates*, G.I. Dzhardimalieva and I. E. Uflyand, Editors. 2018, Springer International Publishing: Cham. p. 633-759.
40. Hubab, M. and M.A. Al-Ghouti, Recent advances and potential applications for metal-organic framework (MOFs) and MOFs-derived materials: Characterizations and antimicrobial activities. *Biotechnology Reports*, 2024: p. e00837.
41. Mohan, B., et al., Advanced luminescent metal–organic framework (MOF) sensors engineered for urine analysis applications. *Coordination Chemistry Reviews*, 2024. **519**: p. 216090.
42. Zhang, Y., et al., Luminescent sensors based on metal-organic frameworks. *Coordination Chemistry Reviews*, 2018. **354**: p. 28-45.
43. Su, W., et al., Challenges and recent advances in MOF-based gas separation membranes. *Chemical Communications*, 2024.
44. Vikal, A., et al., Exploring metal-organic frameworks (MOFs) in drug delivery: A concise overview of synthesis approaches, versatile applications, and current challenges. *Applied Materials Today*, 2024. **41**: p. 102443.
45. Khalid, M., S. Kamal, and S.A. Akmal, Chapter 9 - Solubility and thermodynamic stability of metal–organic frameworks, in *Synthesis of Metal-Organic Frameworks Via Water-based Routes*, Y. Azim, et al., Editors. 2024, Elsevier. p. 159-178.
46. Deng, Y., et al., Prospects, advances and biological applications of MOF-based platform for the treatment of lung cancer. *Biomaterials Science*, 2024. **12**(15): p. 3725-3744.
47. Yang, J. and Y.-W. Yang, Metal-organic framework-based cancer theranostic nanoplatfoms. *VIEW*, 2020. **1**(2): p. e20.
48. Miyah, Y., et al., MOF-derived magnetic nanocomposites as potential formulations for the efficient removal of organic pollutants from water via adsorption and advanced oxidation processes: A review. *Materials Today Sustainability*, 2024: p. 100985.
49. Maya, F., et al., Magnetic solid-phase extraction using metal-organic frameworks (MOFs) and their derived carbons. *TrAC Trends in Analytical Chemistry*, 2017. **90**: p. 142-152.

50. Sun, T., et al., Metal organic frameworks derived single atom catalysts for electrocatalytic energy conversion. *Nano Research*, 2019. **12**(9): p. 2067-2080.
51. Radwan, A., et al., Design engineering, synthesis protocols, and energy applications of MOF-derived electrocatalysts. *Nano-Micro Letters*, 2021. **13**: p. 1-32.
52. Aamer, I., et al., Synthesis, characterization and CO₂ adsorption studies of DABCO based pillared Zn-BDC and Co-BDC metal organic frameworks. *Materials Research Express*, 2021. **8**(7): p. 075506.
53. Li, P., et al., Amino-modified mesoporous carbon material for CO₂ adsorption in tunnel engineering: materials characterization and application prospects. *Case Studies in Construction Materials*, 2024. **20**: p. e02940.
54. Aftab, L., et al., Synthesis, characterization and gas adsorption analysis of solvent dependent Zn-BTC metal organic frameworks. *Separation Science and Technology*, 2021. **56**(13): p. 2159-2169.
55. Cassani, M.C., et al., A Cu (ii)-MOF based on a propargyl carbamate-functionalized isophthalate ligand. *RSC advances*, 2021. **11**(33): p. 20429-20438.
56. Asghar, A., et al., Efficient electrochemical synthesis of a manganese-based metal–organic framework for H₂ and CO₂ uptake. *Green Chemistry*, 2021. **23**(3): p. 1220-1227.
57. Cendrowski, K., et al., The river water influence on cationic and anionic dyes collection by nickel foam with carbonized metal–organic frameworks and carbon nanotubes. *Journal of Alloys and Compounds*, 2021. **876**: p. 160093.
58. Chen, Y., et al., Separation of propylene and propane with pillar-layer metal–organic frameworks by exploiting thermodynamic-kinetic synergetic effect. *Chemical Engineering Journal*, 2022. **431**: p. 133284.
59. Ding, H.-J., et al., Defective hierarchical pore engineering of a Zn–Ni MOF by labile coordination bonding modulation. *Inorganic Chemistry*, 2021. **60**(7): p. 5122-5130.
60. Alhussainy, J.Y., R.T.A. Alrubaye, and R. Th, Gas Adsorption and Storage at Metal-Organic Frameworks. *Journal of Engineering*, 2022. **28**(1).
61. Chen, C., et al., Microwave-assisted synthesis of bimetallic NiCo-MOF-74 with enhanced open metal site for efficient CO₂ capture. *Environmental Functional Materials*, 2022. **1**(3): p. 253-266.

62. Pirzadeh, K., et al., CO₂ and N₂ adsorption and separation using aminated UiO-66 and Cu₃(BTC)₂: A comparative study. *Korean Journal of Chemical Engineering*, 2020. **37**: p. 513-524.
63. Schulte, Z.M., et al., H₂/CO₂ separations in multicomponent metal-adeninate MOFs with multiple chemically distinct pore environments. *Chemical Science*, 2020. **11**(47): p. 12807-12815.
64. Zhang, Y., et al., Studies on the removal of phosphate in water through adsorption using a novel Zn-MOF and its derived materials. *Arabian Journal of Chemistry*, 2022. **15**(8): p. 103955.
65. Khan, J., et al., Isonicotinic acid-based copper-MOF: An exotic redox propertied electrode material for high energy asymmetric supercapacitor. *Journal of Energy Storage*, 2023. **72**: p. 108655.
66. Zhang, Q., et al., Construction of triazine-heptazine-based carbon nitride heterojunctions boosts the selective photocatalytic C–C bond cleavage of lignin models. *Applied Catalysis B: Environmental*, 2023. **331**: p. 122688.
67. Chen, F., et al., Carbon dioxide capture in gallate-based metal-organic frameworks. *Separation and Purification Technology*, 2022. **292**: p. 121031.
68. Azhar, M.H., et al., CO₂ adsorption properties of Ni-BDC MOF and its 1–8 wt% g-C₃N₄/Ni-BDC MOF. *Materials Science and Engineering: B*, 2024. **299**: p. 117043.
69. Ul-Hamid, A., *A Beginners' Guide to Scanning Electron Microscopy*. 2018: Springer International Publishing.
70. Waseda, Y., E. Matsubara, and K. Shinoda, *X-Ray Diffraction Crystallography: Introduction, Examples and Solved Problems*. 2011: Springer Berlin Heidelberg.
71. Smith, B.C., *Fundamentals of Fourier Transform Infrared Spectroscopy*. 2011: CRC Press.
72. Menczel, J.D. and R.B. Prime, *Thermal Analysis of Polymers: Fundamentals and Applications*. 2009: Wiley.
73. Walls, J.M., *Methods of Surface Analysis: Techniques and Applications*. 1990: Cambridge University Press.
74. Rackley, S.A., *Carbon Capture and Storage*. 2009: Butterworth-Heinemann.

75. Mohammadi, T., et al., Monitoring of ethanol electrooxidation on highly efficient conductive RuNi metal-organic framework by mass spectrometry. *Journal of Power Sources*, 2024. **611**: p. 234758.
76. Bhuyan, A. and M. Ahmaruzzaman, Ultrasonic-assisted synthesis of highly efficient and robust metal oxide QDs immobilized-MOF-5/Ni-Co-LDH photocatalyst for sunlight-mediated degradation of multiple toxic dyes. *Journal of Alloys and Compounds*, 2024. **972**: p. 172781.
77. Asghar, A., et al., Efficient One-Pot Synthesis of a Hexamethylenetetramine-Doped Cu-BDC Metal-Organic Framework with Enhanced CO₂ Adsorption. *Nanomaterials*, 2019. **9**(8): p. 1063.
78. Mohammadi, T., et al., One-step growth of RuNi-MOF nanoarrays on carbon felt host as a high-performance binder-free electrode for dual application: Ethanol fuel cell and supercapacitor. *Journal of Energy Storage*, 2024. **79**: p. 110146.
79. Panda, J., et al., Experimental and DFT study of transition metal doping in a Zn-BDC MOF to improve electrical and visible light absorption properties. *The Journal of Physical Chemistry C*, 2022. **126**(30): p. 12348-12360.
80. Sadeghi, S., M. Montazer, and F. Dadashian, Insights into the hexamine-assisted ZnO based-MOFs formation on PET fabric for improved self-cleaning, flame retardant, and hydrophilic properties. *Progress in Organic Coatings*, 2024. **192**: p. 108458.
81. de Jesus, J.R., et al., Successful synthesis of eco-friendly Metal-Organic framework ([Ni (BDC)]_n) allows efficient extraction of multiresidues pesticides and dyes from fish samples. *Microchemical Journal*, 2024. **201**: p. 110592.
82. Mguni, L.L., et al., Modulated synthesized Ni-based MOF with improved adsorptive desulfurization activity. *Journal of Cleaner Production*, 2021. **323**: p. 129196.
83. Wang, J., et al., A highly efficient Co-based catalyst fabricated by coordination-assisted impregnation strategy towards tandem catalytic functionalization of nitroarenes with various alcohols. *Journal of Catalysis*, 2021. **404**: p. 462-474.
84. Feng, W., et al., Wet chemistry synthesis of ZnO crystals with hexamethylenetetramine(HMTA): Understanding the role of HMTA in the formation of ZnO crystals. *Materials Science in Semiconductor Processing*, 2016. **41**: p. 462-469.
85. Ju, Y., et al., An ultrathin Zn-BDC MOF nanosheets functionalized polyacrylonitrile composite separator with anion immobilization and Li⁺

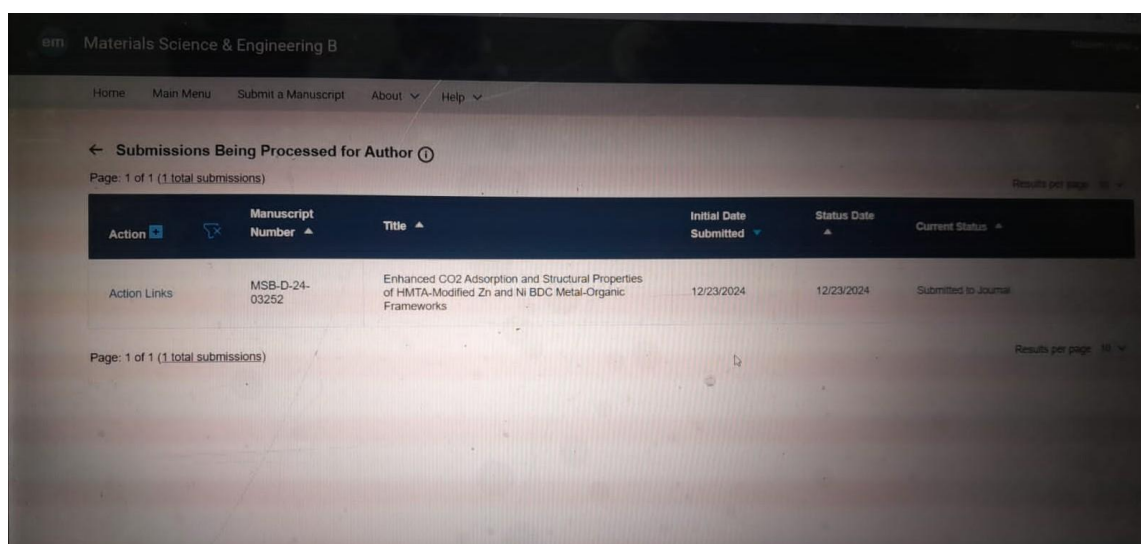
- redistribution for dendrite-free Li metal battery. *Composites Communications*, 2023. **37**: p. 101449.
86. Riaz, S. and S.-J. Park, Thermal and Mechanical Interfacial Behaviors of Graphene Oxide-Reinforced Epoxy Composites Cured by Thermal Latent Catalyst. *Materials*, 2019. **12**(8): p. 1354.
 87. Usman, M., et al., Advanced strategies in metal-organic frameworks for CO₂ capture and separation. *The Chemical Record*, 2022. **22**(7): p. e202100230.
 88. Wang, S., et al., Hierarchical porous N-doped carbon xerogels for high performance CO₂ capture and supercapacitor. *Colloids and Surfaces A: Physicochemical and Engineering Aspects*, 2021. **616**: p. 126285.
 89. Chang, H., et al., Single-Layer 2D Ni–BDC MOF Obtained in Supercritical CO₂-Assisted Aqueous Solution. *Chemistry – A European Journal*, 2022. **28**(61): p. e202201811.
 90. Haris Azhar, M., et al., CO₂ adsorption properties of Ni-BDC MOF and its 1–8 wt% g-C₃N₄/Ni-BDC MOF. *Materials Science and Engineering: B*, 2024. **299**: p. 117043.
 91. Moghadasnia, M.P., et al., Toward the Next Generation of Permanently Porous Materials: Halogen-Bonded Organic Frameworks. *Crystal Growth & Design*, 2024. **24**(6): p. 2304-2321.

LIST OF PUBLICATIONS

Title: “Enhanced CO₂ Adsorption and Structural Properties of HMTA-Modified Zn and Ni BDC Metal-Organic Frameworks”

Journal: Materials Science & Engineering B

Status: Submitted



em | Materials Science & Engineering B

Home Main Menu Submit a Manuscript About Help

← Submissions Being Processed for Author

Page: 1 of 1 (1 total submissions) Results per page: 10

Action	Manuscript Number	Title	Initial Date Submitted	Status Date	Current Status
Action Links	MSB-D-24-03252	Enhanced CO ₂ Adsorption and Structural Properties of HMTA-Modified Zn and Ni BDC Metal-Organic Frameworks	12/23/2024	12/23/2024	Submitted to Journal

Page: 1 of 1 (1 total submissions) Results per page: 10